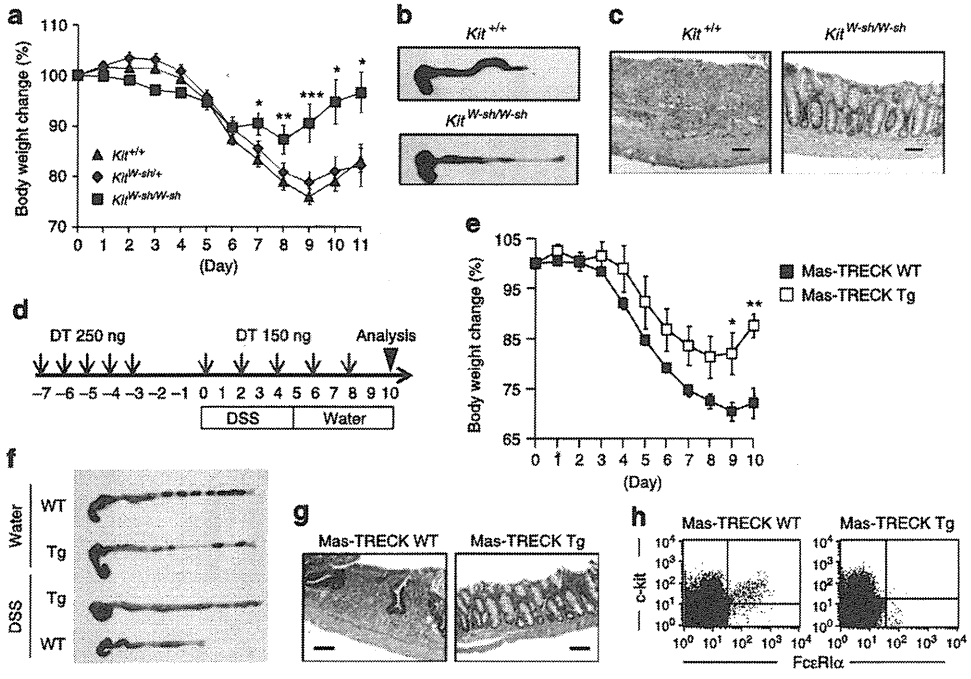

Figure 2 | Impaired DSS-induced colitis in MC-deficient mice. $Kit^{W\text{-}sh/W\text{-}sh}$ MC-deficient, $Kit^{+/+}$ control mice and Mas-TRECK transgenic (Tg) mice were subjected to DSS-induced colitis. (**a**) Body weight changes are shown as percentages of the baseline value and are means±s.e.m. ($n=22$ for $Kit^{+/+}$; $n=25$ for $Kit^{W\text{-}sh/+}$; $n=10$ for $Kit^{W\text{-}sh/W\text{-}sh}$). $^{*}P<0.01$, $^{**}P=0.0207$ and $^{***}P=0.0004$ (two-tailed Student's *t*-test). (**b**,**c**) Eleven days after DSS treatment, colon tissue and haematoxylin and eosin (H&E)-stained tissue sections were examined. Data are representative of at least three independent experiments. (**d**) Mas-TRECK Tg mice and their wild-type (WT) littermates were subjected to DSS-induced colitis. For diphtheria toxin (DT) treatment, mice were injected intraperitoneally with 250 ng of DT for 5 consecutive days (black arrows) and then with 150 ng every other day (red allows). (**e**) Body weight changes are shown as percentages of the baseline value and are means±s.e.m. ($n=6$ for Tg; $n=10$ for WT), $^{*}P=0.0107$, $^{**}P=0.0037$ (two-tailed Student's *t*-test). (**f**) Representative images of whole colons 10 days after DSS treatment. (**g**) Representative images of H&E staining. Scale bars, 100 μm. (**h**) Representative flow cytometric data of infiltrated c-kit^{+} FcεRIα^{+} MCs in the colon.

We next analysed whether the MCs in UC or CD patients expressed P2X7. Although increased number of MCs were observed in the colons of both UC and CD patients (Fig. 1c,d), P2X7 purinoceptors were expressed by the MCs in CD patients but not by those in UC patients or healthy volunteers (Fig. 5g,h). Thus, it is likely that P2X7 purinoceptor-mediated MC activation also occurs in the human colon, especially in CD patients.

To examine whether ATP was extracellularly released at high concentrations at inflammatory sites, we next measured ATP release from inflammatory colonic tissues. An elevated level of ATP release from the colon tissue was noted in TNBS-treated mice (Fig. 6a). In addition, intrarectal administration of non-hydrolyzable ATP (adenosine 5′-*O*-(3-thio) triphosphate and *O*-(4-benzoyl)benzoyl adenosine 5′-triphosphate) led to MC activation in the colonic tissue, similar to the effect of TNBS treatment (Fig. 6b). In contrast, intrarectal administration of other P2Y receptor agonists did not increase colonic MC activation (Fig. 6b). These findings indicate that inflammatory stimuli induce the extracellular release of ATP, which in turn leads to P2X7-dependent MC activation in the colon and subsequent exacerbation of intestinal inflammation.

P2X7 signalling activates the caspase-1 inflammasome to induce the production of IL-1β and IL-18 (ref. 25). IL-1β production is also mediated by MC proteases, such as chymases[26]. We therefore examined whether MCs produced IL-1β via P2X7 receptor activation, and if so whether this production was caspase-1-dependent. IL-1β production was decreased when P2X7-deficient MCs were stimulated with ATP, whereas substantial amounts of IL-1β were produced in caspase-1-deficient MCs (Supplementary Fig. S6), indicating that IL-1β production was P2X7-dependent but caspase-1-independent. In line with this finding, body weight changes were noted in $Kit^{W\text{-}sh/W\text{-}sh}$ mice reconstituted with *caspase-1*$^{-/-}$ MCs (Fig. 5a). These results suggest that MC-dependent inflammation through P2X7 purinoceptors is not dependent on caspase-1-mediated IL-1β or IL-18 production.

An autocrine loop of ATP conversion mediates MC activation. In addition to ATP, other nucleotides (for example, extracellular ADP) act as signals to induce inflammatory responses[27]. We confirmed that MCs are activated by high concentrations of ADP and ATP (Fig. 7a,b). Extracellular ATP is hydrolysed by ectonucleoside triphosphate diphosphohydrolases (CD39) to ADP and AMP; it is then further hydrolysed by ecto-5′-nucleotidase (CD73) to adenosine, which has anti-inflammatory functions[27]. Colonic MCs expressed CD39 but not CD73 (Supplementary Fig. S7a,b), indicating that MCs can convert ATP to ADP but not to adenosine. We therefore examined the involvement of ADP-reactive P2Y purinoceptors and found that P2Y1 and P2Y12 were highly expressed on colonic MCs (Fig. 7c). However, inhibitors of P2Y1 and P2Y12 receptors, as well as knockdown of the P2Y12 receptor, had no effect on the induction of CD63^{+}-activated MCs (Fig. 7d,e; Supplementary Fig. S8a). Similarly, intestinal inflammation, as well as activation of colonic MCs, was unaffected in clopidogrel (a P2Y12 receptor inhibitor)-treated mice (Supplementary Fig. S8b–d). These data indicate that although P2Y1 and P2Y12 were expressed on MCs neither P2Y1 nor P2Y12 purinoceptors mediate ADP-dependent CD63^{+} MC induction.

It is generally accepted that P2X7 purinoceptors specifically recognize ATP[7], but we found that they were also involved in ADP-mediated MC activation. Indeed, no activation was noted in *P2x7*$^{-/-}$ MCs when they were stimulated with ADP (Fig. 7f), leading us to hypothesize that ADP promotes ATP release from MCs and their subsequent stimulation. To test this hypothesis, we measured the expression of pannexin-1, connexin 43 and connexin 32, which

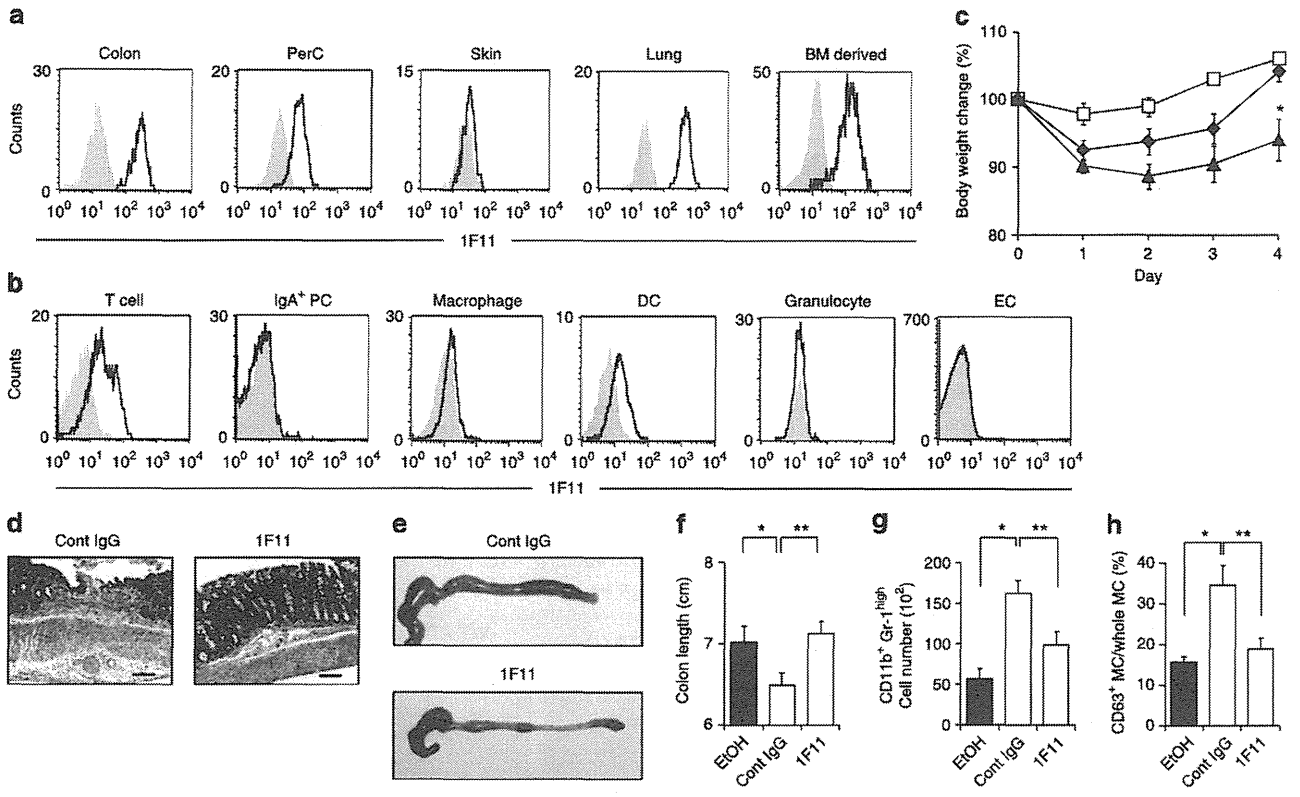

Figure 3 | Amelioration of colitis by treatment with intestinal MC-reactive 1F11 mAb. (**a**) MCs in the colonic lamina propria, peritoneal cavity (PerC), skin and lung, as well as BM-derived MCs, were stained with 1F11 mAb. Control staining with rat IgG2b is shown in grey. (**b**) Cells were isolated from colonic lamina propria and epithelium. $CD3^+$ T cells, IgA^+ plasma cells (PCs), $F4/80^+$ macrophages, $CD11c^+$ DCs, $Gr1^+$ granulocytes and ECs were gated and their reactivity to 1F11 mAb examined. Control staining with rat IgG2b is shown in grey. (**c**) C57BL/6 mice were treated with TNBS and their body weights were monitored for 4 days; 0.5 mg of 1F11 or the control mAb was intraperitoneally administered. Data from 9 (EtOH; open squares), 19 (TNBS with control mAb; closed triangles) and 12 (TNBS with 1F11 mAb; closed diamonds) mice. $^*P = 0.0066$ (Welch's *t*-test). Data are shown as percentages of baseline weights and are means ± s.e.m. (**d**,**e**) Representative images of haematoxylin and eosin staining and colon tissue from 1F11 mAb-treated mice. Scale bars, 100 μm. (**f**) Colon length was measured 4 days after TNBS administration. $^*P = 0.0445$; $^{**}P = 0.0073$ (two-tailed Student's *t*-test). (**g**) Neutrophils ($CD11b^+$ $Gr\text{-}1^{high}$) were quantified as percentages and numbers of cells. Data are shown as means ± s.e.m. ($n = 6$), $^*P < 0.0001$, $^{**}P = 0.0047$ (two-tailed Student's *t*-test). (**h**) Percentage of $CD63^+$ MCs in all c-kit$^+$ FcεRIα$^+$ MCs was determined with flow cytometry. Data are shown as means ± s.e.m. ($n = 6$) $^*P = 0.0202$; $^{**}P = 0.0284$ (two-tailed Student's *t*-test).

are ATP-releasing hemichannels, during cell activation[28,29]. The hemichannels were rarely expressed on the colonic MCs (Fig. 7g), and no inhibitory effect was observed when the MCs were treated with ADP in the presence of hemichannel inhibitors (flufenamic acid and carbenoxolone). However, cell activation was inhibited by P2X7 antagonists [oxidized ATP (OxATP), pyridoxal-phosphate-6-azophenyl-2′,4′-disulfonate and 4,4′-diisothiocyanatostilbene-2,2′-disulfonic acid disodium salt hydrate] (Fig. 7h). To further exclude the possibility that ADP triggers ATP release, we stimulated MCs with another P2Y ligand (UTP); we found that UTP did not induce MC activation (Fig. 7b).

We then tested whether ADP was converted to ATP by ATP-converting enzymes such as ecto-adenylate kinase, ATP synthase and nucleoside diphosphokinase[30]. To test the involvement of these enzymes, we used inhibitors of ecto-adenylate kinase (diadenosine pentaphosphate; AD2P5), ATP synthase (oligomycin; oligo) and nucleoside diphosphokinase (UDP), and we found that inhibition of ecto-adenylate kinase and ATP synthase, but not nucleoside diphosphokinase, reduced ADP- as well as ATP-dependent MC activation (Fig. 7h,i). Neither AD2P5 nor oligo inhibited MC activation induced by the crosslinking of IgE with relevant allergen (Fig. 7i). Among the adenylate kinases, adenylate kinase 1 (AK1) and AK2 were expressed in colonic MCs, and the expression of AK2 was much higher than that of AK1 (Supplementary Fig. S9a). As with AD2P5 treatment, knockdown of AK2, but not AK1, led to the inhibition of both ADP- and ATP-mediated MC activation (Supplementary Fig. S9b). These results indicate that P2X7 purinoceptors have an important role in the activation of MCs by ATP, including ATP derived from ADP by the action of ecto-enzymes such as ATP synthase and AK2.

Neutrophil infiltration by MC-derived mediators. Evaluation of MC activation on the basis of CD63 expression is an important criterion[13]; however, degranulation is not absolutely associated with cytokine production[31]. Therefore, we measured MC production of an array of inflammatory cytokine, chemokine and lipid mediators to additionally elucidate the role of P2X7 purinoceptor-mediated MC activation in the development of intestinal inflammation. Stimulation of MCs with ATP induced the production of inflammatory cytokines such as IL-6, tumour necrosis factor (TNF)α and oncostatin M[32]; this induction was not observed in *P2x7*$^{-/-}$ MCs or in wild-type MCs treated with 1F11 mAb (Fig. 8a,b).

We showed that neutrophil infiltration into the colon was mediated by MC activation (Fig. 1h,i), and a previous study suggested that neutrophil infiltration is a potential target in colitis treatment[33]. Consistent with these findings, ATP stimulation induced MCs, but not *P2x7*$^{-/-}$ MCs, to produce leukotrienes (LTs; LT C4/D4/E4), which are associated with the translocation of 5-lipoxygenase (5-LO) into the nucleus—an important step for LT synthesis in MCs[34] (Fig. 8c,d). Also, chemokine gene array analysis demonstrated that

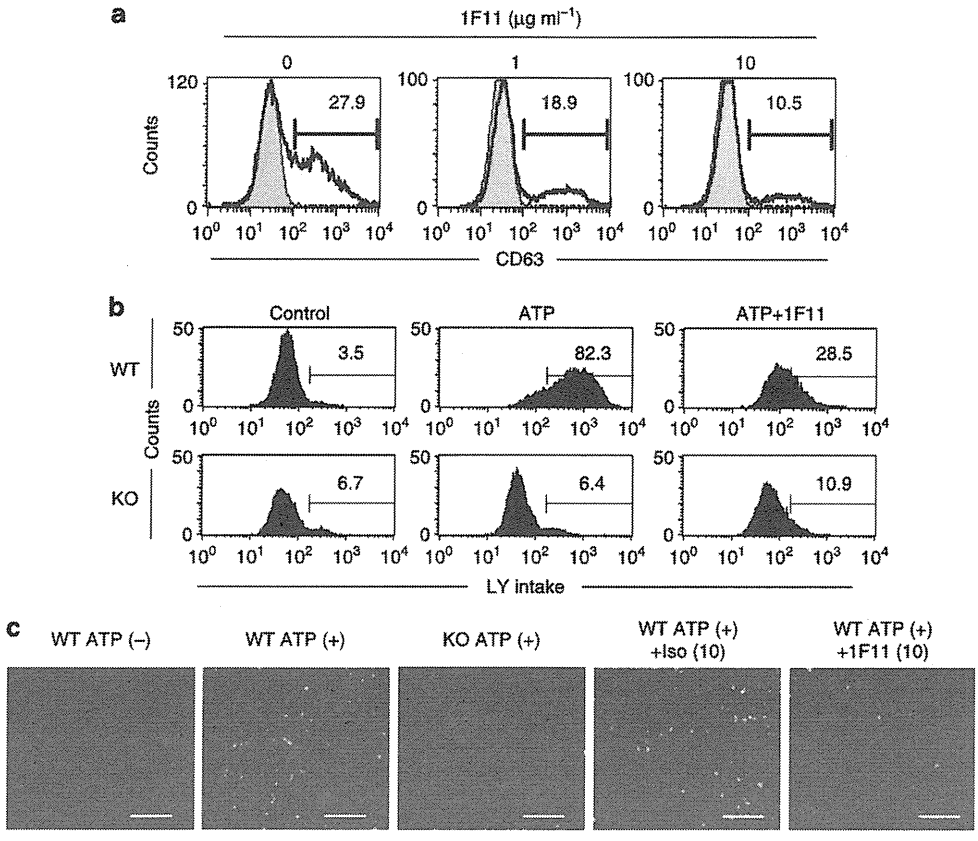

Figure 4 | Inhibition of *in vitro* ATP-mediated MC activation by 1F11 mAb. (**a**) BM-derived MCs, pretreated with various concentrations of 1F11 mAb (0, 1, 10 μg ml^{-1}) for 15 min, were stimulated with 0.5 mM ATP for 30 min. Cells were stained with an anti-CD63 mAb for flow cytometric analysis. Data are representative of three independent experiments. (**b**) BM-derived MCs pretreated with various concentrations of 1F11 mAb or control rat IgG2b (0, 10 μg ml^{-1}) for 15 min were stimulated with 0.5 mM ATP for 30 min in the presence of 1 mg ml^{-1} Lucifer yellow (LY). (**c**) LY uptake was determined by using flow cytometry and fluorescence microscopy. Scale bar, 100 μm. Data are representative of three individual experiments.

ATP stimulation of MCs induced the expression of chemokines, including CCL2, CCL7 and CXCL2 (Fig. 8e–g), and 1F11 mAb treatment or P2X7 deficiency resulted in decreased CCL2 production from MCs activated by ATP but not by IgE plus allergen (Fig. 8g). Furthermore, *Kit*$^{W\text{-}sh/W\text{-}sh}$ mice showed decreased levels of both CCL2 and IL-1β in the colon tissue, but the production levels of these molecules recovered when the mice were reconstituted with wild-type MCs (Supplementary Fig. S10a). As neutrophils express the corresponding chemokine receptors, it is likely that ATP-dependent MC activation induced inflammatory neutrophil infiltration into the colon from the peripheral blood (Supplementary Fig. S10b,c), given the high level of TNFα production by the neutrophils (Supplementary Fig. S10d). These results indicate that ATP-dependent MC activation has key roles in the induction of inflammatory responses (by inducing inflammatory cytokines) and in the exacerbation of inflammatory responses (by inducing LTs and chemokines to recruit TNFα-producing neutrophils to the colon).

Discussion

Here, we showed that MCs have a critical role in the severity of colitis through their interaction with ATP and P2X7 purinoceptors. These interactions not only induce MC-mediated inflammatory responses but also exacerbate them by promoting neutrophil infiltration. Indeed, MC-deficient mice reconstitution with wild-type, but not *P2x7*$^{-/-}$, MCs resulted in neutrophil infiltration and severe inflammatory responses, together with increased production of IL-1β, LTs and CCL2 (Figs 5 and 8, and Supplementary Fig. S10). *Kit*$^{Wsh/Wsh}$ mice spontaneously show elevated levels of neutrophils in their spleens[35]; however, we confirmed that the neutrophil levels were the same as those in the colons of *Kit*$^{+/+}$, *Kit*$^{Wsh/+}$ and *Kit*$^{Wsh/Wsh}$ mice under naïve conditions (Fig. 1h,i). To exclude the possible involvement of other immunological defects in *Kit*$^{Wsh/Wsh}$ mice, such as the involvement of the *Corin* gene, which is associated with type II transmembrane serine protease[35], we further confirmed the amelioration of intestinal inflammation in conditional MC-deficient mice (Fig. 2d–h). These findings strongly suggest that P2X7 on MCs has a pivotal role in the development of murine and human intestinal inflammation.

P2X7 purinoceptors are expressed on T cells, DCs, macrophages and ECs[9–11,25,36]. In a recent study, ATP/P2X7-mediated signalling inhibited the generation and function of regulatory T cells and ATP stimulation led to their conversion into Th17 cells via an IL-6-dependent pathway; thus, the P2X7 antagonist OxATP inhibited colitis[37]. In that study, ATP/P2X7-mediated regulation of regulatory T cells was involved in the chronic phase of intestinal inflammation, which takes about 4 weeks for disease development[37]. Similarly, ATP-mediated DC activation occurs in the chronic phase of intestinal inflammation through the preferential induction of Th17 cells, although whether this is mediated by P2X7 remains to be seen[38]. In contrast, ATP/P2X7-mediated MC activation in our model was important in the development of T-cell-independent acute colitis, which occurs within 1 week. Thus, our study and those of others[37,38] complement each other by reflecting the complicated pathological aspects and kinetics of the acute and chronic phases of intestinal inflammation mediated by ATP and P2X7.

We also found that the expression level of P2X7 receptors differed depending on the tissue and animal species. First, colonic MCs expressed high levels of P2X7, but skin MCs did not

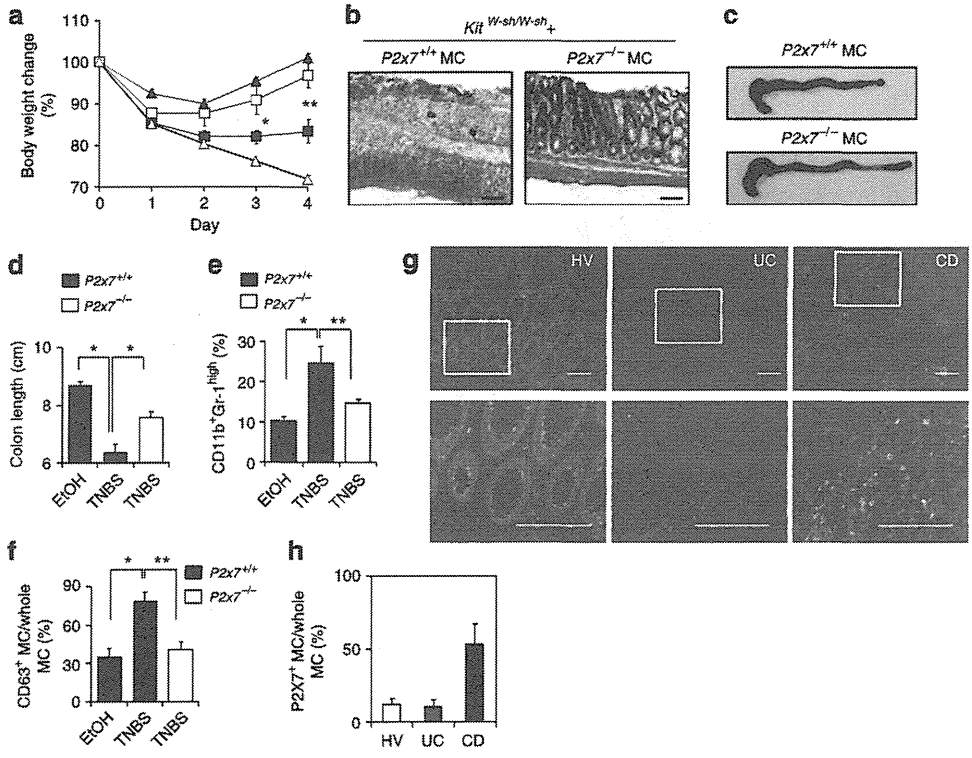

Figure 5 | Inhibitory targeting of P2X7 purinoceptors on MCs leads to amelioration of colonic inflammation. *Kit*$^{W\text{-}sh/W\text{-}sh}$ MC-deficient mice reconstituted with *P2x7*$^{+/+}$, *P2x7*$^{-/-}$ or *caspase-1*$^{-/-}$ BM-derived MCs were applied to a TNBS-induced colitis model. (**a**) Body weight changes were monitored in TNBS-treated *Kit*$^{W\text{-}sh/W\text{-}sh}$ mice reconstituted with *P2x7*$^{+/+}$ (closed squares; $n=9$), *P2x7*$^{-/-}$ (open squares; $n=7$) or *caspase-1*$^{-/-}$ (open triangles; $n=4$). BM-derived MCs were used for TNBS treatment, and *P2x7*$^{+/+}$ BM-derived MC-reconstituted *Kit*$^{W\text{-}sh/W\text{-}sh}$ mice receiving EtOH served as controls (closed triangles; $n=3$). $^{*}P=0.0264$ (two-tailed Student's *t*-test), $^{**}P=0.0058$ (two-tailed Student's *t*-test). Data are shown as percentages of baseline weights and are means±s.e.m. (**b**) Representative images of haematoxylin and eosin staining are shown. Scale bars represents 100 μm. (**c**) Representative images of whole colons are shown. (**d**) Colon length was measured 4 days after TNBS administration. Data are shown as means±s.e.m. ($n=3$ for *P2x7*$^{+/+}$ EtOH, $n=9$ for *P2x7*$^{+/+}$ TNBS, $n=7$ for *P2x7*$^{-/-}$ TNBS), $^{*}P<0.001$ (two-tailed Student's *t*-test). (**e**) Representative flow cytometric data of infiltrated neutrophils (CD11b^{+}Gr-1^{high}) in the colon from three individual experiments. $^{*}P=0.00741$, $^{**}P=0.0009$ (two-tailed Student's *t*-test). Data are shown as means±s.e.m. (**f**) The percentage of CD63^{+} MCs in all c-kit^{+} FcεRIα^{+} MCs was determined with flow cytometry. Data are shown as means±s.e.m. ($n=3$–9), $^{*}P=0.007$ (Welch's *t*-test), $^{**}P=0.0234$ (Welch's *t*-test). (**g**) Colonic tissue sections from a healthy volunteer (HV) and from UC and CD patients were stained with 4′,6-diamidino-2-phenyl indole (blue), MC tryptase (red) and P2X7 (green). Scale bars, 100 μm. (**h**) Cells expressing both P2X7 and MC tryptase were counted in the fields of the tissue sections (four fields for each section). Data are means±s.e.m. ($n=6$).

(Fig. 3a). Second, in contrast to MCs, some macrophages (for example, microglia and RAW264.7 cells) expressed higher levels of P2X7 than did colonic macrophages (Fig. 3b and data not shown). Third, among the several types of immunocompetent cell in the colon, MCs expressed the highest levels of P2X7 (Fig. 3a,b). Fourth, we found P2X7 expression on human colonic ECs, but not on murine colonic ECs (Figs 3b and 5g). In addition, as reported previously[36], P2X7 expression on ECs was downregulated in the colons of CD patients; instead, CD patients showed increased numbers of P2X7^{+} MCs in their colons (Fig. 5g,h). It is important to note that, like murine MCs, human lung MCs express functional P2X7 (ref. 39). Therefore, although we must recognize the similarities and differences between mouse and human intestinal inflammation and MC distribution, ATP/P2X7-mediated MC activation seems to have a major role in the development of intestinal inflammation.

We found elevated levels of extracellular ATP in the colons of TNBS-treated mice (Fig. 6a). This high ATP concentration was most likely achieved by a combination or cascade of several ATP production pathways (for example, cell injury or lysis[7], pattern recognition receptor-mediated activation of monocytes[40] and commensal bacteria[38]). In our tissue culture system, we detected elevated release of ATP (40 μM) in the inflamed colon compared with the control (Fig. 6); however, at least 100 μM ATP was required for MC activation *in vitro* in the single cell culture system (Fig. 7b). This disparity likely reflects the differences in the culture conditions. Unlike in the single cell culture system, the concentration of secreted ATP in the tissue culture system could have been diluted in the culture medium, or ATP could have been consumed rapidly by activated inflammatory cells in the tissue. Alternatively, a lack of commensal bacteria-derived ATP in the tissue culture system as a result of the inclusion of antibiotics may have reduced the ATP level. Another possibility is that the abundant endogenous ATP-degrading enzymes (for example, CD39) in the colon tissue may have degraded some of the ATP. In support of this idea, a suppressive role for CD39 in intestinal inflammation has been reported[41].

We found that ADP-reactive P2Y1 and P2Y12 receptors were expressed on colonic MCs (Fig. 7c), but inhibition or knockdown of these receptors did not suppress the CD63 expression (Fig. 7d,e; Supplementary Fig. S8a). In previous studies, stimulation of MCs with ADP (0.05–50 μM) has led to calcium influx via the P2Y1- but not the P2Y12-mediated pathway[42], whereas our results indicate that CD63 expression required a higher concentration of ADP and was not suppressed by a P2Y1 inhibitor (Fig. 7b,d). This finding indicates that P2Y purinoceptors are not involved in the induction of CD63^{+}-activated MCs that is mediated by high concentrations of ADP. However, we found that adenylate kinase and ATP synthase converted ADP back to ATP, which subsequently induced P2X7

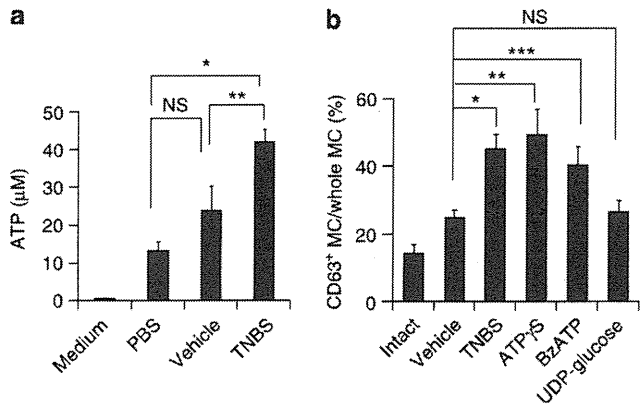

Figure 6 | Enhanced ATP production in intestinal inflammation and MC activation induced by non-hydrolyzable ATP. (**a**) The concentration of ATP released from the colon tissue of mice receiving intrarectally administered phosphate-buffered saline, vehicle or TNBS was measured. Data are shown as means±s.e.m. ($n=3$–7). *$P=0.0004$, **$P=0.0447$ (two-tailed Student's *t*-test). (**b**) CD63 expression of colonic MCs was measured with flow cytometry after intrarectal administration of vehicle ($n=14$), TNBS ($n=5$), non-hydrolyzable ATP (adenosine 5′-O-(3-thio) triphosphate (ATPγS); $n=9$ or O-(4-benzoyl)benzoyl adenosine 5′-triphosphate (BzATP); $n=10$) or UDP-glucose ($n=6$), or in intact mice ($n=7$). Data are shown as means±s.e.m. *$P=0.0002$ (two-tailed Student's *t*-test), **$P=0.0135$ (Welch's *t*-test) and ***$P=0.0238$ (Welch's *t*-test). NS, not significant.

purinoceptor-dependent MC activation. A similar conversion of ADP to ATP has been reported for endothelial cells[27]. Among adenylate kinases, AK2 was highly expressed on MCs and had a pivotal role in the conversion of ADP to ATP (Supplementary Fig. S9a,b). As another P2Y ligand (UTP) did not induce MC activation (Fig. 7b), our findings suggest that ADP could be converted into ATP by AK2 and ATP synthase, and that this ATP subsequently activates MCs through P2X7 purinoceptors. In addition, colonic MCs do not express ecto-5′-nucleotidase (CD73), an enzyme that degrades ADP into adenosine, which has anti-inflammatory effects in intestinal inflammation[43]. Therefore, our study indicates that MCs express CD39, adenylate kinases and ATP synthase, but not CD73, to preferentially convert ADP to ATP for the exacerbation of inflammatory responses through P2X7 purinoceptors.

Here, we showed that colitis aggravated by P2X7-mediated activation of MCs was independent of the inflammasome pathway, and that P2X7-mediated activation of MCs promoted TNFα production by effector cells to further promote intestinal inflammation[44]. Our findings also suggest that MCs exacerbate inflammation by recruiting neutrophils to produce abundant TNFα, but less IL-10 than is produced by other cells (for example, eosinophils, DCs and macrophages; Supplementary Fig. S10d). This neutrophil recruitment was mediated by the production of IL-1β, LTs and chemokines, which are potential targets for the treatment of colitis. Mice with experimentally induced colitis that lack CXCR2 or 5-LO (a key enzyme for converting arachidonic acid to LTs), as well as mice treated with inhibitors of CCR2, CXCR2 or 5-LO, show reduced inflammation and less neutrophil recruitment in their colons[33,45,46]. Moreover, given that ATP promotes neutrophil migration[47], it is possible that P2X7-dependent LT and chemokine production, as well as ATP generation via AK2 and ATP synthase from MCs, could amplify neutrophil infiltration of the colon. These data collectively indicate that MCs are key factors in the induction of intestinal inflammation and also recruit neutrophils to heighten inflammatory responses. P2X7-dependent MC activation could, therefore, be a target for the treatment of intestinal inflammation.

Methods

Mice and human samples. Female C57BL/6 mice were purchased from CLEA Japan. Rag1$^{-/-}$ and P2x7$^{-/-}$ mice were obtained from Jackson Laboratory (Bar Harbour, ME, USA). MC-deficient *Kit*$^{W\text{-}sh/W\text{-}sh}$ mice were obtained from Dr H. Suto (Atopy Research Center, Juntendo University, Japan). For the conditional MC-deficient analysis, Mas-TRECK tg mice were injected intraperitoneally with 250 ng of diphtheria toxin for 5 consecutive days and then with 150 ng every other day[18]. *Caspase-1*$^{-/-}$ mice were backcrossed with C57BL/6 mice; F5 mice were used for this experiment[48]. All mice were maintained under specific-pathogen-free conditions at the Experimental Animal Facility of the Institute of Medical Science, the University of Tokyo. All experiments were approved by the Animal Care and Use Committee of the University of Tokyo.

MC reconstitution was performed as described previously[49]. Briefly, BM-derived MCs were obtained from *P2x7*$^{+/+}$, *P2x7*$^{-/-}$ or *caspase-1*$^{-/-}$ mice as described previously[22]. BM-derived MCs (5×10^6) were intravenously transferred to *Kit*$^{W\text{-}sh/W\text{-}sh}$ mice at two time points (0 and 14 days). The reconstituted mice were used 3 months after the last transfer.

Colon specimens from UC and CD patients and healthy volunteers were obtained by endoscopic biopsy at Osaka University Hospital. All subjects provided written informed consent, and the study protocol was approved by the Ethics Committee of Osaka University Graduate School of Medicine (no. 08243) and the Institute of Medical Science, The University of Tokyo (no. 20-67-0331).

Experimental colitis. For TNBS-induced colitis, anaesthetized mice (18–22 g) were sensitized with 2.5% TNBS (Sigma-Aldrich) together with acetone and olive oil[50]. After 1 week, after a 3-h fast, the mice were given 100 μl of 2.5% TNBS in 50% ethanol via a flexible feeding tube that maintained their heads in a vertical position for 10 min. The control group received only 50% ethanol. Weight changes were recorded daily, and tissues were collected for histological analysis and isolation of mononuclear cells from the colonic lamina propria. For mAb treatment, mice were injected intraperitoneally with 0.5 mg of mAb (1F11 or an isotype control) 1 day before being given TNBS/EtOH intrarectally. mAb administration was continued for 3 days. For P2Y12 inhibition with clopidogrel sulphate, (Wako, Osaka, Japan), mice received clopidogrel (0.5 mg ml^{-1}) in their drinking water from 3 days before intrarectal administration of TNBS/EtOH until the end of the study[50]. For DSS-induced colitis, mice were given 3.5% DSS (Wako, for C57BL/6) or 2.5% DSS (MP Biomedicals, Illkirch, France, for Mas-TRECK tg mice) in their drinking water for 5 days and their body weights were monitored daily[50]. In some experiments, non-hydrolysable ATP (adenosine 5′-*O*-(3-thio) triphosphate and *O*-(4-benzoyl)benzoyl adenosine 5′-triphosphate) or UDP-glucose (0.25 mg in 50% EtOH) was intrarectally administered and the effects were analysed 2 days later.

***In vitro* MC stimulation and inhibition.** BM-derived MCs (2.5×10^5) were cultured with various concentrations of adenosine, ADP, ATP, UTP or anti-DNP-IgE with DNP-human serum albumin. Adenosine-3-phosphate 5-phosphosulfate (0.25 mM), carbenoxolone (10 μM), flufenamic acid (100 μM), pyridoxal-phosphate-6-azophenyl-2′,4′-disulfonate (100 μM), 4,4′-diisothiocyanatostilbene-2,2′-disulfonic acid disodium salt hydrate (100 μM), OxATP (0.5 mM), AD2P5 (1 mM), oligo (10 or 100 μM) or UDP (100 μM) was added to the cells for the inhibition assay[27,28,40,51]. All reagents were purchased from Sigma-Aldrich (St Louis, MO, USA, purity was ≥95%). 5-LO (BD Pharmingen, Franklin Lakes, NJ, USA) was stained after permeabilization with 0.2% Triton-X100 for 10 min; nuclei were stained with 4′,6-diamidino-2-phenyl indole.

Cell preparation and flow cytometry. ECs and lamina propria mononuclear cells were isolated from the colon, as described previously[52]. For flow cytometric analysis, cells were incubated with 5 μg ml^{-1} of an anti-CD16/32 antibody (10 μg ml^{-1}, Fc block, BD Pharmingen) for 5 min and stained for 30 min at 4 °C with fluorescence-labeled Abs specific for c-kit (0.2 μg ml^{-1}), Gr-1 (0.4 μg ml^{-1}), CD4 (1 μg ml^{-1}), CD11b (0.2 μg ml^{-1}), CD11c (0.4 μg ml^{-1}), CD39 (0.4 μg ml^{-1}), CD45 (0.4 μg ml^{-1}), IgA (10 μg ml^{-1}), B220 (0.4 μg ml^{-1}; BD Pharmingen), CCR3 (2 μg ml^{-1}), CXCR2 (4 μg ml^{-1}; R&D Systems, Minneapolis, MN, USA), FcεRIα (0.4 μg ml^{-1}), CD73 (0.4 μg ml^{-1}), TLR2 (10 μg ml^{-1}; eBioscience, San Diego, CA, USA), F4/80 (20 μg ml^{-1}), CCR2 (10 μg ml^{-1}), P2X7 (Hano43; 2 μg ml^{-1},Serotec, UK) or CCR1 (10 μg ml^{-1}, Abnova, Taiwan). Flow cytometric analysis and cell sorting were performed by using FACSCalibur and FACSAria (BD Biosciences, Franklin Lakes, NJ, USA), respectively. Sorted cells were stained with May-Giemsa stain in some experiments. Colonic MCs and BM-derived MCs were prepared as described elsewhere[22].

Establishment of an anti-P2X7 mAb (1F11) and an anti-CD63 mAb. The procedure used to establish MC-specific mAbs is shown as a flowchart in Supplementary Figure S3. Briefly, c-kit$^+$ FcεRIα$^+$ MCs were obtained as described previously[22] from the colons of mice that exhibited allergic diarrhoea. Purified colonic MCs (10^6 cells) were injected into the footpads of Sprague Dawley rats seven times, as described previously[53]. Lymphocytes were isolated from the spleen and inguinal lymph nodes and fused with P3X63-AG8.653 myeloma cells (CRL-1580; American Type Culture Collection, Manassas, VA, USA). The reactivity of each hybridoma to the colonic MCs was examined by means of flow cytometry. To identify antigens

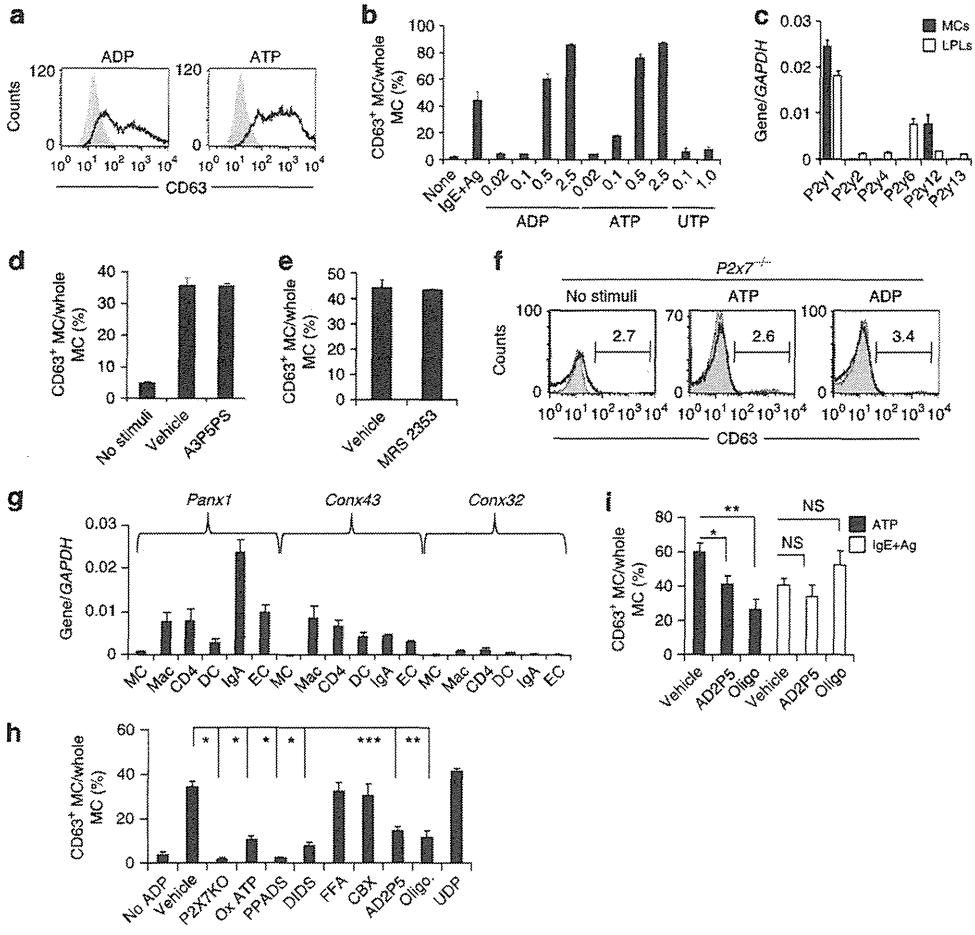

Figure 7 | The ecto-adenylate kinase pathway mediates ADP-dependent MC activation through P2X7 purinoceptors. (**a**) BM-derived MCs treated with ADP or ATP at 0.5 mM for 30 min and examined for CD63 expression. (**b**) BM-derived MCs treated with IgE plus relevant allergen or various concentrations of ADP, ATP or UTP for the analysis of CD63 expression. Data are representative of four experiments. (**c**) Expression of mRNA encoding each P2Y receptor in colonic lamina propria lymphocytes (LPLs) and MCs was analysed by quantitative reverse transcription (RT)-PCR ($n=3$). (**d**,**e**) BM-derived MCs pre-treated with 0.25 mM P2Y1 inhibitor (adenosine-3-phosphate 5-phosphosulfate (A3P5PS)) (**d**) or 0.01 mM P2Y12 inhibitor (MRS2353) (**e**), stimulated with ADP and examined for CD63 expression ($n=3$). (**f**) BM-derived MCs from *P2x7*$^{-/-}$ mice stimulated with ATP or ADP; CD63 expression was determined with flow cytometry. Data are representative of four experiments. (**g**) Expression of pannexin-1 (Panx1), connexin-43 (Conx43) and Conx32 on colonic MCs, macrophages (Mac), CD4$^+$ T cells (CD4), DCs, IgA$^+$ cells (IgA) and ECs was measured by quantitative RT-PCR ($n=4$). (**h**) BM-derived MCs were pretreated with inhibitors of P2X receptors [OxATP, 0.5 mM; pyridoxal-phosphate-6-azophenyl-2′,4′-disulfonate (PPADS); 4,4′-diisothiocyanatostilbene-2,2′-disulfonic acid (DIDS)], connexins [flufenamic acid (FFA)], Panx-1 [carbenoxolone (CBX)], ecto-adenylate kinase [diadenosine pentaphosphate (AD2P5)], ATP synthase (oligomycin) or nucleoside diphosphokinase (UDP) and subsequently stimulated with 0.25 mM ADP. CD63 expression was determined with flow cytometry. ($n=3$) $^*P<0.01$, $^{**}P<0.05$ (two-tailed Student's *t*-test). All data are shown as means±s.e.m. (**i**) BM-derived MCs were treated with AD2P5, oligomycin or UDP and stimulated with 0.5 mM ATP or IgE plus allergen. CD63 expression was determined with flow cytometry ($n=5$). $^*P<0.0001$ (two-tailed Student's *t*-test), $^{**}P=0.0008$ (two-tailed Student's *t*-test) and $^{***}P=0.0008$ (Welch's *t*-test). NS, not significant.

recognized by the mAbs, immunoprecipitation was performed with the mAbs, followed by Liquid chromatography–mass spectrometry analysis, as described previously[53]. Antigen specificity was confirmed by transfecting CHO cells with plasmids that encoded the murine P2X7 receptor and CD63.

Measurements of membrane permeability and inflammatory mediators. To assess membrane permeability, BM-derived MCs were washed twice with phosphate-buffered saline (PBS) and incubated with 1 mg ml^{-1} Lucifer yellow (Sigma-Aldrich) containing 250 μM sulfinpyrazone (Sigma-Aldrich). The MCs were then stimulated with 0.5 mM ATP (Sigma-Aldrich) for 15 min, as described elsewhere[12]. In the inhibition assay, 1 or 10 μg ml^{-1} of 1F11 mAb or the control antibody (Rat IgG2b) was added before ATP stimulation. The fluorescence signal of Lucifer yellow was determined by using fluorescence microscopy (BZ9000, Keyence, Osaka, Japan) and flow cytometry.

To measure the production of cytokines, chemokines and LTs from MCs, BM-derived MCs (2.5×10^5) were stimulated with 2.5 mM ATP for 30 min, after which the supernatants were collected. Chemokine and cytokine production was detected with an inflammatory cytokine kit (BD Pharmingen). For IL-1β measurement, BM-derived MCs from wild-type, *P2x7*$^{-/-}$ and *caspase-1* $^{-/-}$ mice were stimulated with 0.1 μg ml^{-1} of LPS for 4 h, followed by ADP or ATP stimulation. LT C4/D4/E4 production was detected by use of an enzyme-linked immunosorbent assay (GE Healthcare Bio-Science, NJ, USA). For ATP, cytokine and chemokine measurements from the colon tissue, the colon tissues were isolated from mice 2 days after intrarectal administration of TNBS. Released ATP was measured by culturing colon tissues at 100 mg of tissue per 100 μl of RPMI1640 medium for 3 h and using a luminescence ATP detection system (PerkinElmer, Norwalk, CT, USA).

Immunoprecipitation and western blotting. Cell lysates obtained from BM-derived MCs or CHO transfectants (mouse P2X7 variants a, c and d and flag-mP2X7s, cloned from C57BL/6 mice) were analysed by western blotting and immunoprecipitation with 1F11 mAb or the control Ab. Membranes were probed with an anti-flag and a polyclonal rabbit anti-P2X7 antibody (Sigma-Aldrich).

Histology. Colonic tissues were fixed in 4% paraformaldehyde and embedded in paraffin. Tissue sections (5 μm) were stained with haematoxylin and eosin solution, as described previously[22]. For the detection of MCs and P2X7

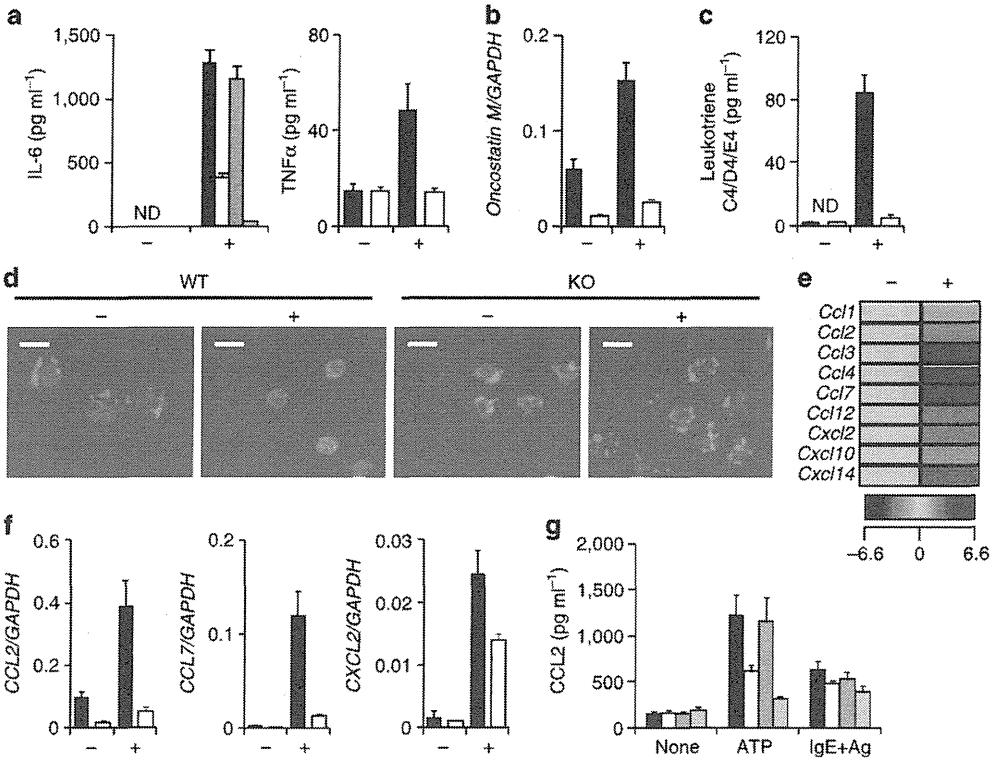

Figure 8 | Critical role of the intestinal MC-associated ATP-P2X7 purinoceptor pathway for induction of neutrophil infiltration. $P2x7^{+/+}$ and $P2x7^{-/-}$ BM-derived MCs were treated with 0.25 mM ATP (+) or left untreated (−). (**a**) Production of IL-6 (left panel; isotype mAb-treated MC, closed column; 1F11 mAb-treated MC, open column; $P2x7^{+/+}$, grey column; and $P2x7^{-/-}$, beige column) and TNFα (right panel) in culture supernatant ($P2x7^{+/+}$, closed column; $P2x7^{-/-}$, open column) was determined after 24 h stimulation. ND, not detected. Data are shown as means±s.e.m. ($n=3$). (**b**) Oncostatin M mRNA expression was measured 30 min after stimulation of $P2x7^{+/+}$ (closed column) and $P2x7^{-/-}$ (open column) MCs with ATP. Data are shown as means±s.e.m. ($n=3$). (**c**) LT C4/D4/E4 production from ATP-stimulated (+) or -unstimulated (−) $P2x7^{+/+}$ (closed column) or $P2x7^{-/-}$ BM-derived MCs (open column) in culture supernatants was measured by using enzyme-linked immunosorbent assay (ELISA). Data are shown as means±s.e.m. ($n=3$). ND, not detected. (**d**) $P2x7^{+/+}$ and $P2x7^{-/-}$ BM-derived MCs were stimulated with 0.5 mM ATP. Cells were fixed and stained with an anti-5LO antibody (red) and 4′,6-diamidino-2-phenyl indole (blue). Scale bar, 10 μm. Data are representative of two experiments. (**e**) Representative data of a chemokine gene array are shown. Increased levels of each chemokine are shown as a heat map. (**f**) mRNA expression of CCL2 (left), CCL7 (middle) and CXCL2 (right) was measured by using quantitative reverse transcription-PCR. Data are shown as means±s.e.m. ($n=3$). (**g**) CCL2 production was enumerated by using ELISA 24 h after stimulation of BM-derived MCs with ATP or IgE plus antigen (IgE+Ag). Isotype mAb-treated MC, closed column; 1F11 mAb-treated MC, open column; $P2x7^{+/+}$ MC, grey column; and $P2x7^{-/-}$ MC, beige column). Data are shown as means±s.e.m. ($n=3$).

expression in human specimens, colonic tissue sections were stained with antibodies for MC tryptase and P2X7 purinoceptors (Alomone Laboratories, Jerusalem, Israel).

shRNA plasmid construction and lentiviral transduction. For the construction of shRNA expression lentivirus vector plasmids, a series of oligonucleotide pairs were synthesized, as listed below. Each oligo pair was annealed and cloned into pmU6[54]. Each mU6-shRNA cassette was then subcloned into the ΔU3 sequence of the 3′-LTR of the lentivirus vector plasmid pLCG to generate pLCG-shCD63 (sense: 5′-TTTGATTCTTGCTGCATCAACATAGCTTCCTGTCACTATGTTGATGCAG CAAGAATCTTTTTTG-3′, antisense: 5′-AATTCAAAAAAGATTCTTGCTGCA TCAACATAGTGACAGGAAGCTATGTTGATGCAGCAAGAAT-3′), pLCG-shP2Y12 (sense: 5′-TTTGATCTACTAATGATTCTAACTGCTTCCTGTCACAGTTAGAAT CATTAGTAGATCTTTTTTG-3′, antisense: 5′-AATTCAAAAAAGATCTACTAA TGATTCTAACTGTGACAGGAAGCAGTTAGAATCATTAGTAGAT-3′) and pLCG-shAK1 (sense: 5′-TTTGCGAGAAGATTGTACAGAAATGCTTCCTGTCA CATTTCTGTACAATCTTCTCGCTTTTTTG-3′, antisense: 5′-AATTCAAAAAA GCGAGAAGATTGTACAGAAATGTGACAGGAAGCATTTCTGTACAATCTT CTCG-3′) and pLCG-shAK2 (sense: 5′-TTTTGGAGCTAATTGAGAAGAATTGC TTCCTGTCACAATTCTTCTCAATTAGCTCCATTTTTTG-3′, antisense: 5′-AATTCAAAAAATGGAGCTAATTGAGAAGAATTGTGACAGGAAGCA ATTCTTCTCAATTAGCTCC-3′).

To obtain lentivirus-encoding green fluorescent protein (as a reporter gene) and shRNA for CD63, 293FT cells (6×10^5) were transfected with pLP1, pLP2, pLP-VSVG and pLCG-shRNA by using Lipofectamine 2000 (Invitrogen, Carlsbad, CA, USA) as per the manufacturer's protocol (Invitrogen). After 24- and 48-h incubations, lentivirus-encoding shRNA was collected.

BM-derived MCs (1×10^6) or MC/9 cells were transduced with shRNA expression lentivirus stock in the presence of 8 μg ml^{-1} Polybrene (Sigma-Aldrich)[55]. After 24 h, the cells were washed and green fluorescent protein-positive cells were sorted by FACSAria and used for subsequent experiments.

Quantitative real-time-PCR. Total RNA was prepared by using TRIzol (Invitrogen) and reverse transcribed by use of Superscript VILO (Invitrogen), as described. Quantitative reverse transcription–PCR was performed with the LightCycler 480 II (Roche, Mannheim, Germany) and the Universal Probe Library (Roche). Primer sequences are listed in Supplementary Table S1.

Statistical analysis. Statistical analysis was performed by using the unpaired two-tailed Student's *t*-test and Welch's *t*-test. The data are presented as means±s.e.m.

References

1. Abraham, C. & Cho, J. H. Inflammatory bowel disease. *N Engl. J. Med.* **361,** 2066–2078 (2009).
2. Strober, W. & Fuss, I. J. Proinflammatory cytokines in the pathogenesis of inflammatory bowel diseases. *Gastroenterology* **140,** 1756–1767 (2011).
3. Alvarez-Errico, D., Lessmann, E. & Rivera, J. Adapters in the organization of mast cell signaling. *Immunol. Rev.* **232,** 195–217 (2009).
4. Bischoff, S. C. Role of mast cells in allergic and non-allergic immune responses: comparison of human and murine data. *Nat. Rev. Immunol.* **7,** 93–104 (2007).
5. Galli, S. J., Borregaard, N. & Wynn, T. A. Phenotypic and functional plasticity of cells of innate immunity: macrophages, mast cells and neutrophils. *Nat. Immunol.* **12,** 1035–1044 (2011).
6. He, S. H. Key role of mast cells and their major secretory products in inflammatory bowel disease. *World J. Gastroenterol.* **10,** 309–318 (2004).
7. Surprenant, A. & North, R. A. Signaling at purinergic P2X receptors. *Annu. Rev. Physiol.* **71,** 333–359 (2009).

8. Erlinge, D. P2Y receptors in health and disease. *Adv. Pharmacol.* **61,** 417–439 (2011).
9. Wilhelm, K. *et al.* Graft-versus-host disease is enhanced by extracellular ATP activating P2X7R. *Nat. Med.* **16,** 1434–1438 (2010).
10. Weber, F. C. *et al.* Lack of the purinergic receptor P2X(7) results in resistance to contact hypersensitivity. *J. Exp. Med.* **207,** 2609–2619 (2010).
11. Muller, T. *et al.* A potential role for P2X7R in allergic airway inflammation in mice and humans. *Am. J. Respir. Cell Mol. Biol.* **44,** 456–464 (2011).
12. Sudo, N. *et al.* Extracellular ATP activates mast cells via a mechanism that is different from the activation induced by the cross-linking of Fc receptors. *J. Immunol.* **156,** 3970–3979 (1996).
13. Furuno, T., Teshima, R., Kitani, S., Sawada, J. & Nakanishi, M. Surface expression of CD63 antigen (AD1 antigen) in P815 mastocytoma cells by transfected IgE receptors. *Biochem. Biophys. Res. Commun.* **219,** 740–744 (1996).
14. Rijnierse, A., Koster, A. S., Nijkamp, F. P. & Kraneveld, A. D. Critical role for mast cells in the pathogenesis of 2,4-dinitrobenzene-induced murine colonic hypersensitivity reaction. *J. Immunol.* **176,** 4375–4384 (2006).
15. Kaser, A., Zeissig, S. & Blumberg, R. S. Inflammatory bowel disease. *Annu. Rev. Immunol.* **28,** 573–621 (2010).
16. Feyerabend, T. B. *et al.* Cre-mediated cell ablation contests mast cell contribution in models of antibody- and T cell-mediated autoimmunity. *Immunity* **35,** 832–844 (2011).
17. Otsuka, A. *et al.* Requirement of interaction between mast cells and skin dendritic cells to establish contact hypersensitivity. *PLoS One* **6,** e25538 (2011).
18. Sawaguchi, M. *et al.* Role of mast cells and basophils in IgE responses and in allergic airway hyperresponsiveness. *J. Immunol.* **188,** 1809–1818 (2012).
19. Fiorucci, S. *et al.* Importance of innate immunity and collagen binding integrin α1β1 in TNBS-induced colitis. *Immunity* **17,** 769–780 (2002).
20. Yoshimoto, T. & Nakanishi, K. Roles of IL-18 in basophils and mast cells. *Allergol. Int.* **55,** 105–113 (2006).
21. Pastorelli, L. *et al.* Epithelial-derived IL-33 and its receptor ST2 are dysregulated in ulcerative colitis and in experimental Th1/Th2 driven enteritis. *Proc. Natl Acad. Sci. USA* **107,** 8017–8022 (2010).
22. Kurashima, Y. *et al.* Sphingosine 1-phosphate-mediated trafficking of pathogenic Th2 and mast cells for the control of food allergy. *J. Immunol.* **179,** 1577–1585 (2007).
23. Nicke, A. *et al.* A functional P2X7 splice variant with an alternative transmembrane domain 1 escapes gene inactivation in P2X7 knock-out mice. *J. Biol. Chem.* **284,** 25813–25822 (2009).
24. Smart, M. L. *et al.* P2X7 receptor cell surface expression and cytolytic pore formation are regulated by a distal C-terminal region. *J. Biol. Chem.* **278,** 8853–8860 (2003).
25. Di Virgilio, F. Liaisons dangereuses: $P2X_7$ and the inflammasome. *Trends Pharmacol. Sci.* **28,** 465–472 (2007).
26. Mizutani, H., Schechter, N., Lazarus, G., Black, R. A. & Kupper, T. S. Rapid and specific conversion of precursor interleukin 1β (IL-1β) to an active IL-1 species by human mast cell chymase. *J. Exp. Med.* **174,** 821–825 (1991).
27. Yegutkin, G. G. Nucleotide- and nucleoside-converting ectoenzymes: important modulators of purinergic signalling cascade. *Biochim. Biophys. Acta.* **1783,** 673–694 (2008).
28. Locovei, S., Bao, L. & Dahl, G. Pannexin 1 in erythrocytes: function without a gap. *Proc. Natl Acad. Sci. USA* **103,** 7655–7659 (2006).
29. Kang, J. *et al.* Connexin 43 hemichannels are permeable to ATP. *J. Neurosci.* **28,** 4702–4711 (2008).
30. Burrell, H. E. *et al.* Human keratinocytes release ATP and utilize three mechanisms for nucleotide interconversion at the cell surface. *J. Biol. Chem.* **280,** 29667–29676 (2005).
31. Foger, N. *et al.* Differential regulation of mast cell degranulation versus cytokine secretion by the actin regulatory proteins Coronin1a and Coronin1b. *J. Exp. Med.* **208,** 1777–1787 (2011).
32. Salamon, P. *et al.* Human mast cells release oncostatin M on contact with activated T cells: possible biologic relevance. *J. Allergy Clin. Immunol.* **121,** 448–455 e5 (2008).
33. Bento, A. F. *et al.* The selective nonpeptide CXCR2 antagonist SB225002 ameliorates acute experimental colitis in mice. *J. Leukoc. Biol.* **84,** 1213–1221 (2008).
34. Luo, M., Jones, S. M., Peters-Golden, M. & Brock, T. G. Nuclear localization of 5-lipoxygenase as a determinant of leukotriene B4 synthetic capacity. *Proc. Natl Acad. Sci. USA* **100,** 12165–12170 (2003).
35. Nigrovic, P. A. *et al.* Genetic inversion in mast cell-deficient *Wsh* mice interrupts corin and manifests as hematopoietic and cardiac aberrancy. *Am. J. Pathol.* **173,** 1693–1701 (2008).
36. Cesaro, A. *et al.* Amplification loop of the inflammatory process is induced by P2X7R activation in intestinal epithelial cells in response to neutrophil transepithelial migration. *Am. J. Physiol. Gastrointest Liver Physiol.* **299,** G32–G42 (2010).
37. Schenk, U. *et al.* ATP inhibits the generation and function of regulatory T cells through the activation of purinergic P2X receptors. *Sci. Signal* **4,** ra12 (2011).
38. Atarashi, K. *et al.* ATP drives lamina propria T_H17 cell differentiation. *Nature* **455,** 808–812 (2008).
39. Wareham, K., Vial, C., Wykes, R. C., Bradding, P. & Seward, E. P. Functional evidence for the expression of P2X1, P2X4 and P2X7 receptors in human lung mast cells. *Br. J. Pharmacol.* **157,** 1215–1224 (2009).
40. Piccini, A. *et al.* ATP is released by monocytes stimulated with pathogen-sensing receptor ligands and induces IL-1β and IL-18 secretion in an autocrine way. *Proc. Natl Acad. Sci. USA* **105,** 8067–8072 (2008).
41. Friedman, D. J. *et al.* From the Cover: CD39 deletion exacerbates experimental murine colitis and human polymorphisms increase susceptibility to inflammatory bowel disease. *Proc. Natl Acad. Sci. USA* **106,** 16788–16793 (2009).
42. Feng, C., Mery, A. G., Beller, E. M., Favot, C. & Boyce, J. A. Adenine nucleotides inhibit cytokine generation by human mast cells through a Gs-coupled receptor. *J. Immunol.* **173,** 7539–7547 (2004).
43. Louis, N. A. *et al.* Control of IFN-αA by CD73: implications for mucosal inflammation. *J. Immunol.* **180,** 4246–4255 (2008).
44. Rijnierse, A., Koster, A. S., Nijkamp, F. P. & Kraneveld, A. D. TNF-α is crucial for the development of mast cell-dependent colitis in mice. *Am. J. Physiol. Gastrointest. Liver Physiol.* **291,** G969–G976 (2006).
45. Cuzzocrea, S. *et al.* 5-Lipoxygenase modulates colitis through the regulation of adhesion molecule expression and neutrophil migration. *Lab. Invest.* **85,** 808–822 (2005).
46. Waddell, A. *et al.* Colonic eosinophilic inflammation in experimental colitis is mediated by $Ly6C^{high}$ $CCR2^{+}$ inflammatory monocyte/macrophage-derived CCL11. *J. Immunol.* **186,** 5993–6003 (2011).
47. Chen, Y. *et al.* Purinergic signaling: a fundamental mechanism in neutrophil activation. *Sci. Signal* **3,** ra45 (2010).
48. Kuida, K. *et al.* Altered cytokine export and apoptosis in mice deficient in interleukin-1β converting enzyme. *Science* **267,** 2000–2003 (1995).
49. Tsai, M., Grimbaldeston, M. A., Yu, M., Tam, S. Y. & Galli, S. J. Using mast cell knock-in mice to analyze the roles of mast cells in allergic responses *in vivo*. *Chem. Immunol. Allergy* **87,** 179–197 (2005).
50. Wirtz, S., Neufert, C., Weigmann, B. & Neurath, M. F. Chemically induced mouse models of intestinal inflammation. *Nat. Protoc.* **2,** 541–546 (2007).
51. Ransford, G. A. *et al.* Pannexin 1 contributes to ATP release in airway epithelia. *Am. J. Respir. Cell Mol. Biol.* **41,** 525–534 (2009).
52. Kunisawa, J. *et al.* Sphingosine 1-phosphate dependence in the regulation of lymphocyte trafficking to the gut epithelium. *J. Exp. Med.* **204,** 2335–2348 (2007).
53. Nochi, T. *et al.* A novel M cell-specific carbohydrate-targeted mucosal vaccine effectively induces antigen-specific immune responses. *J. Exp. Med.* **204,** 2789–2796 (2007).
54. Yu, J. Y., DeRuiter, S. L. & Turner, D. L. RNA interference by expression of short-interfering RNAs and hairpin RNAs in mammalian cells. *Proc. Natl Acad. Sci. USA* **99,** 6047–6052 (2002).
55. Haraguchi, T., Ozaki, Y. & Iba, H. Vectors expressing efficient RNA decoys achieve the long-term suppression of specific microRNA activity in mammalian cells. *Nucleic Acids Res.* **37,** e43 (2009).

Acknowledgements

We thank Drs T. Kitamura and J. Kitaura (The University of Tokyo) for discussions and for providing reagents; Dr H. Suto (Juntendo University) for providing *Kit* $^{W\text{-}sh/W\text{-}sh}$ mice; Dr S. Nakae (The University of Tokyo) for advice on analysing *Kit* $^{W\text{-}sh/W\text{-}sh}$ mice; Drs S. Ohmi, M. Oyama, H. Hata and C. Takamura (The University of Tokyo) for protein analysis; and Dr A. Uozumi, I. Ishikawa and M. Mejima (The University of Tokyo), Drs F. Ishikawa and Y. Saito (RCAI) for technical advice. This work was supported by grants from: the Ministry of Education, Science, Sports and Technology of Japan (Grant-in Aid for Scientific Research S (23229004 to H.K.), for Young Scientists A (22689015 to J.K.), for Scientific Research on Innovative Areas (23116506 to J.K.), for Scientific Research on Priority Areas (19059003 to H.K.), for Challenging Exploratory Research (24659217 to J.K.), Leading-edge Research Infrastructure Program (J.K. and H.K.); the Young Researcher Overseas Visits Program for Vitalizing Brain Circulation of the Japan Society for the Promotion of Science (JSPS; J.K., H.K., Y.K., T.N.), and for JSPS Fellows (021-07124 to Y.K.); the Ministry of Health and Welfare of Japan (J.K. and H.K.); the Global Center of Excellence Program of the Center of Education and Research for Advanced Genome-based Medicine (H.K.); the Program for Promotion of Basic and Applied Research for Innovations in Bio-oriented Industry (BRAIN to J.K.); and the Yakult Bio-Science Foundation (J.K.).

Author contributions

Y.K. conducted the research, performed experiments and wrote the manuscript; T.A. and K.F. performed gene expression and animal experiments; T.N. conducted the mAb experiment; H.T., H. Iba, T.H., M.K. and S.S. contributed to the experimental design and data analysis; S.N. and H. Iijima obtained clinical samples and J.K. and H.K. supervised the project and wrote the manuscript. JK should be contacted for material requests.

Additional information

Supplementary Information accompanies this paper at http://www.nature.com/naturecommunications

Competing financial interests: The authors declare no competing financial interests.

Reprints and permission information is available online at http://npg.nature.com/reprintsandpermissions/

How to cite this article: Kurashima, Y. *et al.* Extracellular ATP mediates mast cell-dependent intestinal inflammation through P2X7 purinoceptors. *Nat. Commun.* 3:1034 doi: 10.1038/ncomms2023 (2012).

THE JOURNAL OF IMMUNOLOGY

The Development of Colitogenic CD4$^+$ T Cells Is Regulated by IL-7 in Collaboration with NK Cell Function in a Murine Model of Colitis

Osamu Yamaji, Takashi Nagaishi, Teruji Totsuka, Michio Onizawa, Masahiro Suzuki, Naoto Tsuge, Atsuhiko Hasegawa, Ryuichi Okamoto, Kiichiro Tsuchiya, Tetsuya Nakamura, Hisashi Arase, Takanori Kanai and Mamoru Watanabe

J Immunol; Prepublished online 13 February 2012;
doi:10.4049/jimmunol.1100371
http://www.jimmunol.org/content/early/2012/02/12/jimmunol.1100371

The Journal of Immunology is published twice each month by
The American Association of Immunologists, Inc.,
9650 Rockville Pike, Bethesda, MD 20814-3994.

Print ISSN: 0022-1767 Online ISSN: 1550-6606.

Published February 13, 2012, doi:10.4049/jimmunol.1100371

The Development of Colitogenic CD4$^+$ T Cells Is Regulated by IL-7 in Collaboration with NK Cell Function in a Murine Model of Colitis

Osamu Yamaji,*,[1] Takashi Nagaishi,*,[1] Teruji Totsuka,* Michio Onizawa,* Masahiro Suzuki,* Naoto Tsuge,* Atsuhiko Hasegawa,[†] Ryuichi Okamoto,* Kiichiro Tsuchiya,* Tetsuya Nakamura,* Hisashi Arase,[‡,§,¶] Takanori Kanai,[‖] and Mamoru Watanabe*

We previously reported that IL-7$^{-/-}$RAG$^{-/-}$ mice receiving naive T cells failed to induce colitis. Such abrogation of colitis may be associated with not only incomplete T cell maintenance due to the lack of IL-7, but also with the induction of colitogenic CD4$^+$ T cell apoptosis at an early stage of colitis development. Moreover, NK cells may be associated with the suppression of pathogenic T cells in vivo, and they may induce apoptosis of CD4$^+$ T cells. To further investigate these roles of NK cells, RAG$^{-/-}$ and IL-7$^{-/-}$RAG$^{-/-}$ mice that had received naive T cells were depleted of NK cells using anti-asialo GM1 and anti-NK1.1 Abs. NK cell depletion at an early stage, but not at a later stage during colitogenic effector memory T cell (T_{EM}) development, resulted in exacerbated colitis in recipient mice even in the absence of IL-7. Increased CD44$^+$CD62L$^-$ T_{EM} and unique CD44$^-$CD62L$^-$ T cell subsets were observed in the T cell-reconstituted RAG$^{-/-}$ recipients when NK cells were depleted, although Fas, DR5, and IL-7R expressions in this subset differed from those in the CD44$^+$CD62L$^-$ T_{EM} subset. NK cell characteristics were the same in the presence or absence of IL-7 in vitro and in vivo. These results suggest that NK cells suppress colitis severity in T cell-reconstituted RAG$^{-/-}$ and IL-7$^{-/-}$RAG$^{-/-}$ recipient mice through targeting of colitogenic CD4$^+$CD44$^+$CD62L$^-$ T_{EM} and, possibly, of the newly observed CD4$^+$CD44$^-$CD62L$^-$ subset present at the early stage of T cell development. *The Journal of Immunology*, **2012, 188: 000–000.**

The pathogenesis of inflammatory bowel diseases (IBD), such as Crohn's disease and ulcerative colitis in humans, is known to be associated with dysregulated immune responses to luminal contents including Ags derived from commensal bacteria in gut. In patients with Crohn's disease, for example, excessive amounts of proinflammatory cytokines, such as IFN-γ, TNF, and IL-17 (1), are secreted predominantly by CD4$^+$ T cells infiltrating colonic tissues. The activities of these cells are thought to reflect the severity of IBD. Additionally, it is known that adoptive transfer of CD4$^+$ naive T cells into lymphopenic immune-deficient animals, such as SCID and RAG$^{-/-}$ mice, induces chronic inflammation in the colon and is considered an animal model of IBD (2, 3).

IL-7 is an important cytokine that is associated with the proliferation of immature B and T cells (4) as well as with homeostatic maintenance of peripheral T cells in vivo (5, 6). We have previously reported that IL-7 is secreted by intestinal epithelia, especially goblet cells (7), and that spontaneous colitis that is similar to IBD in humans is induced in transgenic mice overexpressing IL-7 (8). Additionally, we have shown that the IL-7R^{high}CD4$^+$ T cell subset is pathogenic (9) when the cells are transferred into RAG$^{-/-}$ mice (10, 11). Moreover, we have also shown that adoptive transfer of naive T cells in RAG and IL-7 double-deficient (IL-7$^{-/-}$RAG$^{-/-}$) mice fails to induce colitis (10). Therefore, IL-7 was initially considered to be essential for the induction of colitis. However, it is known that IL-7 is not required for the in vitro differentiation from naive T cells into Th1 or Th17 cells (12). It is also known that the spontaneous proliferation, which is dependent on Ag ligation to the CD3/TCR complex, can be observed even in the T cell-reconstituted IL-7$^{-/-}$RAG$^{-/-}$ re-

*Department of Gastroenterology and Hepatology, Graduate School of Medical Science, Tokyo Medical and Dental University, Tokyo 113-8519, Japan; [†]Department of Immunotherapeutics, Graduate School of Medical Science, Tokyo Medical and Dental University, Tokyo 113-8519, Japan; [‡]Laboratory of Immunochemistry, World Premier International Research Center, Immunology Frontier Research Center, Osaka University, Osaka 565-0871, Japan; [§]Department of Immunochemistry, Research Institute for Microbial Diseases, Osaka University, Osaka 565-0871, Japan; [¶]Japan Science and Technology, Core Research for Evolutional Science and Technology, Saitama 332-0012, Japan; and [‖]Department of Gastroenterology, Keio University School of Medicine, Tokyo 160-8582, Japan

[1]O.Y. and T.N. contributed equally to this work.

Received for publication February 11, 2011. Accepted for publication January 10, 2012.

This work was supported in part by Grants-in-Aid for Scientific Research (to T. Nagaishi, T.T., R.O., K.T., T. Nakamura, T.K., and M.W.), for Scientific Research on Priority Areas (to M.W.), and for Exploratory Research and Creative Scientific Research (to M.W.) from the Japanese Ministry of Education, Culture, Sports, Science, and Technology; the Japanese Ministry of Health, Labor, and Welfare (to M.W.); the Japan Medical Association (to M.W.); the Terumo Life Science Foundation (to M.W.); the Ohyama Health Foundation (to M.W.); the Yakult Bio-Science Foundation (to T.K. and T.T.); the Research Fund of Mitsukoshi Health and Welfare Foundation (to M.W. and R.O.); the Japan Foundation for Applied Enzymology (to M.O.); the Japan Health Sciences Foundation (to M.O.); the Memorial Fund of Nihon University Medical Alumni Association (to T. Nagaishi); the Abbott Japan Allergy Research Award (to T. Nagaishi); the Foundation for Advancement of International Science (to T. Nagaishi); and the Takeda Science Foundation (to T. Nagaishi).

Address correspondence and reprint requests to Dr. Mamoru Watanabe and Dr. Takashi Nagaishi, Department of Gastroenterology and Hepatology, Graduate School of Medical Science, Tokyo Medical and Dental University, 1-5-45 Yushima, Bunkyo-ku, Tokyo 113-8519, Japan. E-mail addresses: mamoru.gast@tmd.ac.jp (M.W.) and tnagaishi.gast@tmd.ac.jp (T.N.)

The online version of this article contains supplemental material.

Abbreviations used in this article: ASGM1, asialo GM1; EAE, experimental autoimmune encephalomyelitis; IBD, inflammatory bowel disease; LP, lamina propria; LPL, lamina propria lymphocyte; PI, propidium iodide; SPL, spleen; T_{EM}, effector memory T cell; WT, wild-type.

www.jimmunol.org/cgi/doi/10.4049/jimmunol.1100371

cipient mice (13, 14). Additionally, our recent studies suggested that effector $CD4^+$ T cells were able to induce colitis even in IL-$7^{-/-}RAG^{-/-}$ mice that were parabiosed with colitic $RAG^{-/-}$ mice that had been injected with naive T cells 6 wk previously (15). Moreover, a deparabiosed IL-$7^{-/-}RAG^{-/-}$ mouse, which was surgically separated from T cell-receiving $RAG^{-/-}$–IL-$7^{-/-}$ $RAG^{-/-}$ parabionts 6 wk after the initial surgery, still maintained chronic colitis for at least another 12 wk (16). These results suggested that the abrogation of colitis in the T cell-reconstituted IL-$7^{-/-}RAG^{-/-}$ mice may be associated with not only incomplete T cell maintenance due to the lack of IL-7, but also with another mechanism by which the colitogenic $CD4^+$ T cell development is suppressed.

It is known that NK cells are responsible for innate immune responses, including the depletion of tumor cells or cells infected with various kinds of viruses (17). Additionally, NK cells induce inflammation in tissues by the production of proinflammatory cytokines such as IFN-γ (18, 19). On the other hand, NK cells are also known to be critical for anti-inflammatory effects in the context of autoimmune diseases (20, 21). It has been reported that NK cells abrogate disease severity of experimental autoimmune encephalomyelitis (EAE) due to the suppression of pathogenic T cells (22, 23). It has also been reported that depletion of NK cells results in enhanced severity of a chronic colitis model (24). However, the mechanisms by which NK cells regulate inflammation in this colitis model have not been well described. In this regard, we hypothesized that the abrogation of colitogenic T cell development that we observed in naive T cell-receiving IL-$7^{-/-}$ $RAG^{-/-}$ mice is associated with the effect of NK cells. We therefore focused our analysis of this phenomenon on NK cells.

Materials and Methods

Animals

Wild-type (WT) C57BL/6 mice were purchased from Japan CLEA (Tokyo, Japan). Rag-deficient ($RAG^{-/-}$) mice on a C57BL/6 background were obtained from Taconic (Hudson, NY) and the Central Laboratories for Experimental Animals (Kanagawa, Japan). IL-$7^{-/-}$ mice were provided by Dr. R. Zamoyska (National Institute for Medical Research, London, U.K.) and were intercrossed with $RAG^{-/-}$ to generate IL-$7^{-/-}RAG^{-/-}$ mice. Mice were maintained under specific pathogen-free conditions in the Animal Care Facility of Tokyo Medical and Dental University. Donors and recipients were used between 8 and 16 wk age. All animal experimentations were approved by the Animal Review Board of Tokyo Medical and Dental University and were performed in accordance with institutional guidelines.

Abs

The following mAbs and reagents were obtained from BD Pharmingen (San Jose, CA): anti-CD3ε (145-2C11), anti-CD4 (RM4-5), anti-CD11b (M1/70), anti-CD11c (HL3), anti-CD27 (LG.3A10), anti-CD28 (37.51), anti-CD43 (S7), anti-CD44 (IM7), anti-CD45RB (16A), anti-CD51 (RMV-7), anti-CD62L (MEL-14), anti-CD69 (H1.2F3), anti-CD94 (18d3), anti-CD95, anti-CD178 (MFL4), anti-CD244.2 (2B4 B6 alloantigen), anti-Ly49C,I (5E6), anti-Ly49D (4E5), anti-Ly49F (HBF-719), anti-Ly49G2 (4D11), anti–IL-7Rα (A7R34), anti-NK1.1 (PK136), and streptavidin. Biotin-conjugated anti-mouse NKG2A/C/E, biotin-conjugated anti-mouse IL-7Rα (A7R34), FITC-conjugated anti-mouse pan-NK cells (CD49b), and FITC-conjugated anti-mouse CD3ε (145-2C11) mAbs were purchased from eBioscience (San Diego, CA).

Flow cytometry (FACS)

To detect the cell surface expression of a variety of molecules, isolated mononuclear cells from individual organs including spleen (SPL), mesenteric lymph node (MLN), and colonic lamina propria (LP) were analyzed by FACS using standard staining methods. Briefly, the cells were suspended in PBS containing 2% FBS, which was used as the suspension fluid for subsequent staining, preincubated with an FcγR-blocking mAb (anti-CD16/32; 2.4G2; BD Biosciences) for 15 min to prevent nonspecific binding by the secondary Ab, and washed with suspension fluid followed by staining with specific FITC-, PE-, PerCP-, allophycocyanin-, or biotin-labeled Abs for 20 min on ice. Standard two-, three-, or four-color flow cytometric analyses were performed using the FACSCalibur (Becton Dickinson, Sunnyvale, CA) with appropriate software (CellQuest; BD Biosciences). Background fluorescence was also assessed by staining with control irrelevant isotype-matched mAbs.

NK cell depletion in vivo

The anti-asialo GM1 (ASGM1) polyclonal Ab was obtained from Wako Chemicals (Osaka, Japan) and reconstituted according to the manufacturer's specifications. The anti-NK1.1 mAb was affinity purified from the culture supernatant of a hybridoma clone, PK136, obtained from the American Type Culture Collection (Manassas, VA). For effective depletion of NK cells in vivo, either the anti-ASGM1 polyclonal Ab (0.25 mg/mouse) or anti-NK1.1 mAb (0.5 mg/mouse) was injected i.p. into mice (25) at the indicated time points in each experiment. The same amount of rabbit Ig (Rockland Immunochemicals, Gilbertsville, PA) or mouse IgG2a (Medical & Biological Laboratories, Nagoya, Japan) were used as the controls, respectively, for some of experiments. Effective (~95%) depletion of NK cells in vivo was confirmed by FACS analysis of single cells derived from individual organs such as SPL, MLN, and colonic LP.

Purification of naive T cell subsets and induction of colitis

For naive T cell purification, splenic mononuclear cells were obtained from WT mice and $CD4^+$ T cells were isolated using anti-CD4 (L3T4) MACS magnetic beads (Miltenyi Biotec, Bergisch Gladbach, Germany) according to the manufacturer's instructions. Enriched $CD4^+$ T cells (94–97% pure as estimated by FACS) were then labeled with PerCP- or allophycocyanin-conjugated anti-CD4, PE- or allophycocyanin-conjugated anti-CD44, and FITC-conjugated anti-CD62L. Subpopulations of $CD4^+$ cells were generated by three-color sorting on a FACSAria (Becton Dickinson). All populations were 98.0% pure on reanalysis. To induce an animal model of chronic colitis, 5×10^5 $CD4^+CD44^-CD62L^+$ (naive) T cells were adoptively transferred i.p. into 8- to 12-wk-old $RAG^{-/-}$ or IL-$7^{-/-}RAG^{-/-}$ recipient mice as previously described (2, 3, 10).

Isolation of LP lymphocytes

LP lymphocytes (LPL) were isolated from healthy or colitic mice as previously described (10). Briefly, $RAG^{-/-}$ or IL-$7^{-/-}RAG^{-/-}$ recipient mice were sacrificed 6–12 wk after injection of naive T cells to induce colitis. The entire length of the colon was removed, opened longitudinally, washed with PBS, and cut into small pieces. The dissected tissues were incubated with Ca^{2+}-, Mg^{2+}-free HBSS containing 1 mM DTT (Sigma-Aldrich, St. Louis, MO) for 45 min to remove mucus, and the epithelial layer was then treated with 3.0 mg/ml collagenase (Roche Diagnostics, Mannheim, Germany) and 0.01% DNase (Worthington Biomedical, Freehold, NJ) for 2 h. The cells were pelleted, washed twice with PBS, and were then subjected to density gradient centrifugation using 40–75% isotonic Percoll (Amersham Biotech, Piscataway, NJ) solution diluted with HBSS. Isolated whole LP mononuclear cells were subjected to FACS to analyze each lymphocyte subset. In some experiments, such LP mononuclear cells were further labeled with allophycocyanin-conjugated anti-CD4 and FITC-conjugated anti-CD3 to isolate colitogenic $CD4^+$ T cell subsets by FACSAria. All populations were 98.0% pure on reanalysis. Isolated LP $CD4^+$ T cells were subjected to cytokine production and cytotoxicity assays.

Determination of clinical score of colitis

The clinical score of colitis was determined using previously described methods (26) with minor modifications and was assessed by trained individuals blinded to the treatment group. Briefly, initial body weight and wasting, hunching over, piloerection, diarrhea, and blood in the stool or per rectum of the T cell-receiving $RAG^{-/-}$ or IL-$7^{-/-}RAG^{-/-}$ recipient mice were assessed when sacrificed. For wasting, weight loss of $<20\%$ from baseline was assigned 0 points and weight loss of $>20\%$ was assigned 1 point. For hunched over appearance, no obvious hunching was assigned 0 point, and extensive hunching was assigned as 1 point. For colon thickening, normal features were assigned 0 points, mild thickening was assigned 1 point, moderate thickening was assigned 2 points, and severe thickening was assigned 3 points. For stool consistency, 0 points were assigned to well-formed pellets, 1 point to pasty and semiformed stools that did not adhere to the anus, and 2 points to liquid stools that did adhere to the anus. An additional point was added if gross blood was noted. The scores of these parameters were added, resulting in a total clinical score ranging from 0 (healthy) to 8 (maximal colitis activity).

Histopathological examination of colitis

Mice receiving naive T cells were sacrificed 6 or 12 wk after the T cell transfer, and colonic specimens taken from proximal, middle, and distal colons were subjected to histopathological assessment. For this assessment, tissue samples were fixed in 10% neutral-buffered formalin. Paraffin-embedded sections (5 μm) were stained with H&E. The H&E-stained sections were analyzed without prior knowledge of the type of donors, recipients, and treatments. The degree of inflammation in the colon was graded according to a modification of the previously described scoring system (26, 27). Briefly, for mucosal damage, 0 points were assigned to normal appearance, 1 point to discrete lymphoepithelial lesions, 2 points to diffuse crypt elongation, and 3 points to extensive crypt elongation or mucosal erosion/ulceration. For cell infiltration the points assigned were: 0, to normal, or presence of occasional leukocytes; 1, to widely scattered leukocytes or focal aggregates of leukocytes; 2, to confluence of leukocytes extending into the submucosa with focal effacement of the muscularis; 3, to transmural extension of leukocyte infiltration. For crypt abscess, the assigned points were: 0, to no crypt abscess; 1, to the presence of crypt abscess. The cumulative degree of these parameters was calculated as a total histological score ranging from 0 (no change) to 21 (extensive cell infiltration and tissue damage).

ELISA

To measure cytokine production, 1×10^5 LP $CD4^+$ T cells were cultured in 200 μl RPMI 1640 (Sigma-Aldrich) supplemented with 10% heat-inactivated FBS, 500 U/ml penicillin, 100 μg/ml streptomycin (Sigma-Aldrich), 10 mM HEPES, 1% nonessential amino acids, and 50 μM 2-ME (Life Technologies Invitrogen, Carlsbad, CA), termed complete RPMI 1640, in the presence of 5 μg/ml plate-bound anti-CD3ε (145-2C11) and 2 μg/ml soluble anti-CD28 (37.51) mAbs on flat-bottom 96-well plates (Costar, Cambridge, MA) at 37°C in a humidified atmosphere incubator containing 5% CO_2 for 48 h. Culture supernatants were removed and analyzed for the production of cytokines such as IFN-γ, TNF, and IL-17. Cytokine concentrations were determined using specific ELISAs (R&D Systems, Minneapolis, MN) as per the manufacturer's recommendations.

Isolation of NK cells and cytotoxicity assay

Spleen cell suspensions were prepared from $RAG^{-/-}$ or IL-$7^{-/-}RAG^{-/-}$ mice and treated with NH_4Cl buffer to remove erythrocytes. The NK cell population was then labeled with FITC-conjugated anti-DX5 (CD49b) and isolated for use as effector cells in the cytotoxicity assay by sorting on a FACSAria. The purity of isolated NK cells was 98.0% on reanalysis. To measure cytokine production, 5×10^4 NK cells were cultured in 200 μl RPMI 1640 supplemented with 10% FBS, 500 U/ml penicillin, and 100 μg/ml streptomycin in the presence of 100 ng/ml rIL-2, 100 ng/ml rIL-12, and 100 ng/ml rIL-18 on flat-bottom 96-well plates at 37°C in a humidified atmosphere incubator containing 5% CO_2. Culture supernatants were removed after 24 h and analyzed for IFN-γ production. Cytotoxicity assays were performed using the flow cytometric method reported by Xu et al. (28; see also Ref. 29). Briefly, isolated naive T cells from WT mice or LP effector memory T cells (T_{EM}) from colitic mice were labeled with a lipophilic green fluorescent cell linker, PKH2 (Sigma-Aldrich), which is incorporated into the plasma membrane. Uniform labeling of cells was confirmed by flow cytometry. Labeled 5×10^4 target T cells were coincubated in round-bottom 96-well plates (Costar) with effector NK cells (T:E ratio, 1:5 to 1:0.6) in complete RPMI 1640 supplemented with 100 ng/ml rIL-2 (PeproTech, London, U.K.) with or without 50 ng/ml rIL-7 (PeproTech) at 37°C in humidified air containing 5% CO_2 for 4 h. Naive T cells or LP colitogenic T cells that were incubated under the same conditions but without effector NK cells were also prepared as controls. Cells were then collected, stained with propidium iodide (PI), and analyzed by FACS. Cytotoxic activity was determined by calculating the percentage of the double-positive population for both PI (FL2) and PKH2 (FL1). In some experiments, a mouse lymphoma cell line, YAC-1, obtained from the American Type Culture Collection, was used as target cells for a [^{51}Cr] release assay with the standard protocol. Briefly, target cells were labeled with 3.7 MBq of $Na_2[^{51}Cr]O_4$ for 1 h at 37°C and washed three times with PBS before mixing (1×10^4/well) with effector cells in round-bottomed 96-well plates at different E:T ratios (1.25:1, 2.5:1, 5:1, 10:1, 20:1) in triplicates. After 4 h incubation, cell-free supernatants were collected and radioactivity measured by MicroBeta counter (Wallac). The percentage of lysis is calculated by (sample release − spontaneous release)/(maximum release − spontaneous release).

Statistical analysis

The results are expressed as the means ± SEM. Statistical significance was determined using the nonparametric Mann–Whitney U test, and differences were considered to be statistically significant when $p < 0.05$.

Results

NK cell depletion induces the early onset of colitis in naive T cell-transferred $RAG^{-/-}$ mice

It has been reported that NK cells suppress the severity of inflammatory diseases such as EAE and colitis (22, 24). NK cells were depleted in the latter colitis study by injection of anti-NK1.1 or anti-ASGM1 Abs, or by the use of a perforin-deficient animal. That study suggested that NK cells may possibly have cytolytic activity for colitogenic $CD4^+$ T_{EM} in this model since knockout of the perforin gene resulted in exacerbation of disease severity. However, it is unclear which stage in the development of colitis is affected by NK cells. Therefore, we first assessed the effect of NK cell depletion at different time points in the development of chronic colitis.

To examine the effect of NK cells in the development of chronic inflammation in the colon, an animal model of colitis was induced by adoptive transfer of $CD4^+CD62L^+D44^-$ (naive) T cells derived from WT SP into $RAG^{-/-}$ recipient mice (2, 3). NK cells were depleted by i.p. injection of the anti-ASGM1 Ab (or vehicle control [PBS]) every other day for 12 wk starting from the day before naive T cell transfer (Fig. 1A). Additionally, some groups were injected with the anti-ASGM1 Ab for 4 wk followed by vehicle control for 8 wk (Fig. 1A), or with the vehicle control for 4 wk followed by 8 wk anti-ASGM1 Ab (Supplemental Fig. 1). Mice injected with the anti-ASGM1 Ab for 12 wk, or for just the first 4 wk, started to show wasting earlier than the vehicle control group that was injected for 12 wk (Fig. 1B). Alternatively, mice injected with vehicle control for 4 wk followed by 8 wk anti-ASGM1 Ab showed a similar wasting curve to that of mice injected with vehicle control for 12 wk (data not shown), suggesting that NK cell depletion at the later stage of colitis induction does not affect the severity of colitis.

However, there was no significant difference in clinical scores between these groups 12 wk after the T cell transfer (Fig. 1C), and all mouse groups showed a similar degree of colitis with thickening and shortening of the colon as well as splenomegaly when sacrificed (Fig. 1D). Consistent with this finding, microscopic evaluation of each group showed similar histopathological features such as wall thickening of the colon, infiltration mainly by mononuclear cells, crypt abscesses, crypt elongation, a decrease in goblet cells, and epithelial damage (Fig. 1E, 1F). Moreover, the production of proinflammatory cytokines by colonic LP T cells isolated from each group was similar (Fig. 1G).

However, there was concern that anti-ASGM1 Ab treatment at an early stage may affect the colitis severity in the $RAG^{-/-}$ mice receiving naive T cells, since the groups with the Ab treatment at an early stage for 4 wk and 12 wk started to exhibit wasting earlier than the control group without the Ab treatment (Fig. 1B). Therefore, we examined these mice at a relatively early time and, interestingly, we found that the Ab-treated group showed significantly more severe colitis in clinical and histological scores compared with the control group 6 wk after T cell transfer (Fig. 2). These data indicate that NK cell depletion affects the early stage of colitis development.

$CD62L^-CD44^+$ and $CD62L^-CD44^-$ T cell subsets are increased by NK cell depletion in naive T cell-reconstituted $RAG^{-/-}$ recipient mice

Because the exacerbation at an early stage of colitis development was observed following NK cell depletion, we assessed the number of $CD4^+$ T cells in SPL and MLN of naive T cell-receiving $RAG^{-/-}$ mice treated with or without the anti-ASGM1 Ab. As seen in Fig. 3A and 3B, increased numbers of T cells were detected, especially

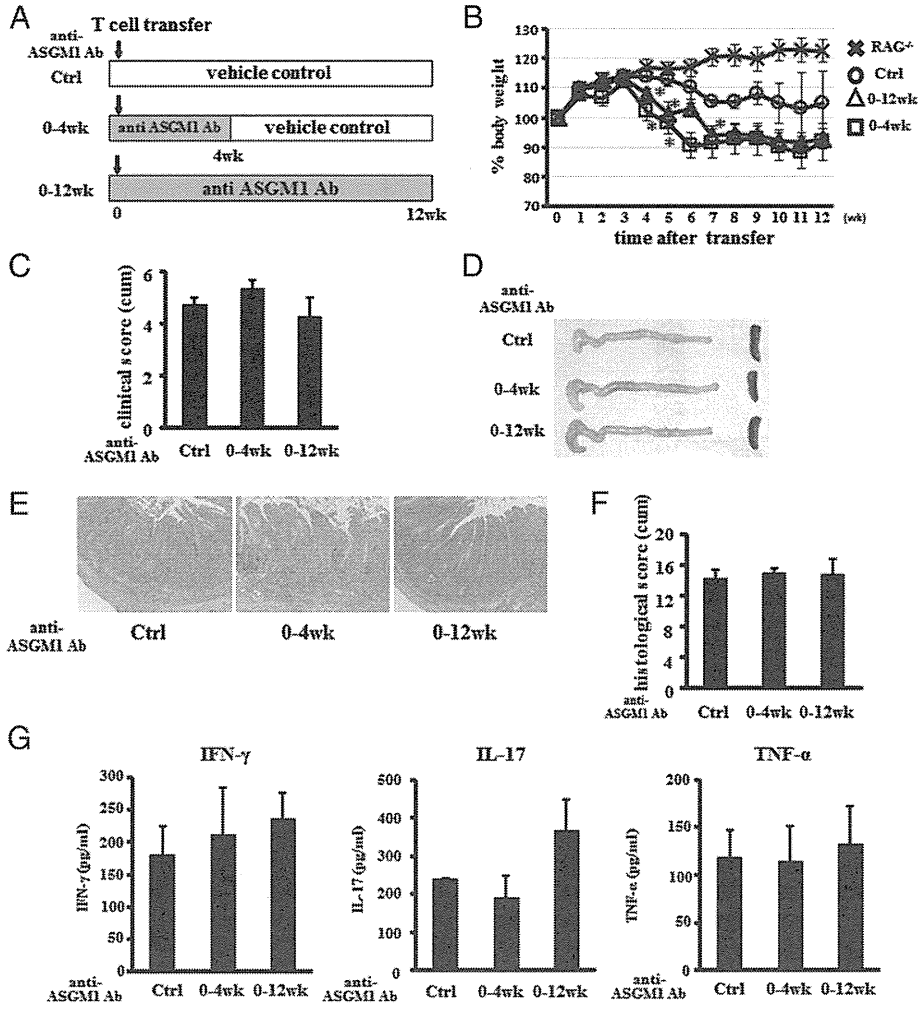

FIGURE 1. NK cell depletion at the early stage of colitis induction in $RAG^{-/-}$ mice results in wasting disease. (**A**) Protocol for NK cell depletion in a chronic colitis setting. $RAG^{-/-}$ mice were injected with either 0.25 mg/mouse anti-ASGM1 Ab (0–12 wk) or vehicle control (Ctrl) every second day for 12 wk from the day before adoptive transfer of naive T cells, or were injected with anti-ASGM1 Ab for 4 wk followed by vehicle control injection for 8 wk (0–4 wk). (**B**) Wasting, as defined by percentage of initial body weight, in $RAG^{-/-}$ mice induced colitis. Mice were injected with naive T cells and either vehicle control for 12 wk (Ctrl, ○), anti-ASGM1 Ab for 12 wk (0–12 wk, △), or anti-ASGM1 Ab for 4 wk followed by 8 wk vehicle control (0–4 wk, □). The non–T cell-injected control group is also shown ($RAG^{-/-}$, cross). Data are expressed as means ± SEM from four mice. $*p < 0.05$. (**C**) Clinical scores of each group are shown. Data are expressed as means ± SEM from four mice. (**D**) Gross appearance of colons (*left*) and SP (*right*) from naive T cell-transferred $RAG^{-/-}$ recipients injected with either vehicle control for 12 wk (Ctrl, *top*), anti-ASGM1 Ab for 4 wk and then control for 8 wk (0–4 wk, *middle*), or anti-ASGM1 Ab for 12 wk (0–12 wk, *bottom*). Representative features from four experiments are shown. (**E**) Histological feature of colons from naive T cell-transferred $RAG^{-/-}$ recipients injected with control for 12 wk (Ctrl, *left*), anti-ASGM1 Ab for 4 wk and then control for 8 wk (0–4 wk, *middle*), or anti-ASGM1 Ab for 12 wk (0–12 wk, *right*). Representative features from each group are shown. (**F**) Histological scores of each group are shown. Data are expressed as means ± SEM from four mice. (**G**) Cytokine production by LP T cells from each group is shown. Concentrations of IFN-γ (*left*), TNF (*middle*), and IL-17 (*right*) in the culture supernatant were measured using ELISA. Data are indicated as means ± SEM from four samples.

in the SPL, within a week after naive T cell injection. Moreover, treatment with the anti-ASGM1 Ab revealed a significantly increased number of T cells in SPL and MLN (Fig. 3A, 3B). Thus, we next determined the development of T_{EM} in these mice by assessment of the expression levels of CD62L and CD44 on T cells. From day 1 to day 3, most T cells still expressed CD62L, but not CD44, regardless of anti-ASGM1 Ab treatment. Interestingly, a $CD62L^{-}CD44^{-}$ subset had appeared in both SPL and MLN by day 5 after treatment with anti-ASGM1 Ab (Fig. 3C–F). This unique T cell subset was significantly increased in the naive T cell-receiving $RAG^{-/-}$ mice treated with anti-ASGM1 Ab, especially in MLN, on days 5 and 7 (Fig. 3F), suggesting that NK cells target this $CD62L^{-}CD44^{-}$ T cell subset upon development of colitogenic $CD62L^{-}CD44^{+}$ T_{EM}.

It is thought that the T_{EM}, but not a naive T cell subset, is targeted by NK cells to regulate excessive immune responses (23, 28). However, our observation indicated that a $CD62L^{-}CD44^{-}$ T cell subset is increased in the absence of NK cells. Therefore, we next assessed the expression levels of several markers, which are associated with NK cell function, on each of the T cell subsets. Splenic $CD62L^{+}CD44^{-}$ (naive, R1; Fig. 4, *left panel*), $CD62L^{-}CD44^{-}$ (R2), and $CD62L^{-}CD44^{+}$ (effector memory, R3) T cell subsets were isolated for FACS analysis from $RAG^{-/-}$ mice that had received naive T cells 5 d previously with anti-ASGM1 Ab treatment the day before T cell reconstitution. The expression of Fas and DR5 in $CD62L^{-}CD44^{+}$ cells was higher than that in $CD62L^{+}CD44^{-}$ T cells (Fig. 4). Interestingly, the expression levels of Fas and DR5 in $CD62L^{-}CD44^{-}$ cells were similar to those of $CD62L^{+}CD44^{-}$, but not of $CD62L^{-}CD44^{+}$. Additionally, the expression level of Qa-1 was similar for all of these T cell subsets (Fig. 4). Furthermore, the expression level of IL-7R/CD127 in $CD62L^{-}CD44^{+}$ cells was similar to that of $CD62L^{+}$

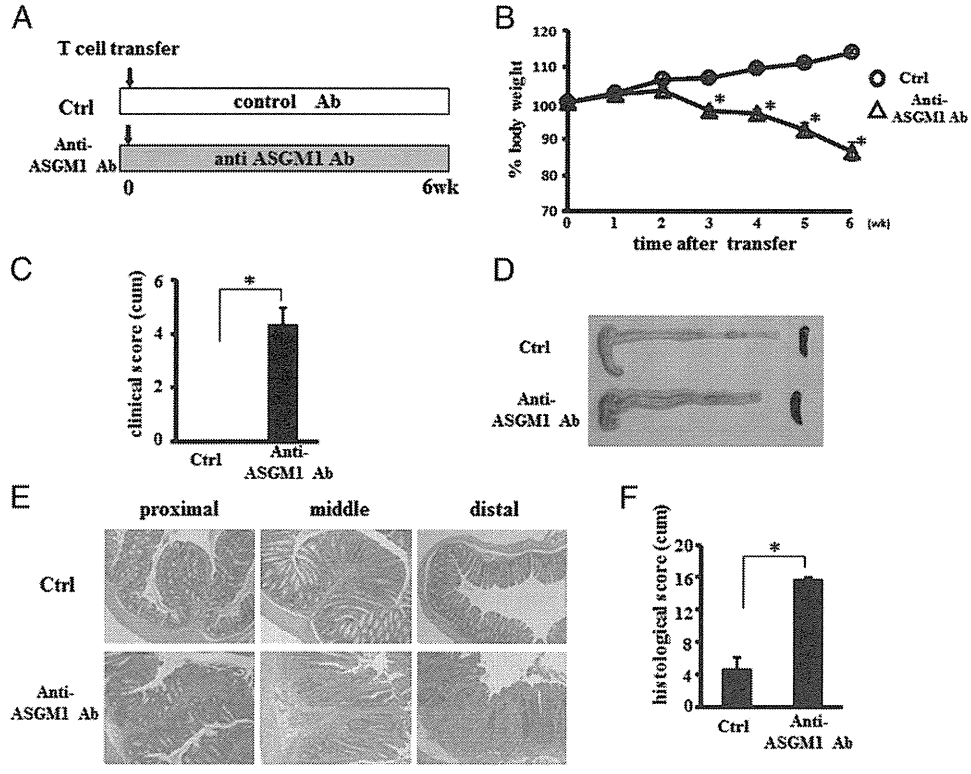

FIGURE 2. NK cell depletion in RAG$^{-/-}$ recipients results in early onset colitis development. (**A**) Protocol for NK cell depletion in a chronic colitis setting. RAG$^{-/-}$ mice were injected with either 0.25 mg/mouse anti-ASGM1 Ab or control IgG every second day for 6 wk from the day before adoptive transfer of naive T cells. (**B**) Wasting, as defined by percentage of initial body weight, in RAG$^{-/-}$ mice induced colitis. Mice were injected with naive T cells with either control IgG (○) or anti-ASGM1 Ab (△) for 6 wk. Data are expressed as means ± SEM from four mice. *$p < 0.05$. (**C**) Clinical scores of each group are shown. Data are expressed as means ± SEM from four mice. *$p < 0.05$. (**D**) Gross appearance of colons (*left*) and SP (*right*) from naive T cell-transferred RAG$^{-/-}$ recipients injected with either control IgG (*top*) or anti-ASGM1 Ab for 6 wk (*bottom*). Representative features from four experiments are shown. (**E**) Histological feature of proximal (*left*), middle (*middle*), and distal (*right*) colons from naive T cell-transferred RAG$^{-/-}$ recipients injected with either control IgG (*top*) or anti-ASGM1 Ab for 6 wk (*botttom*). Representative features from each group are shown. (**F**) Histological scores of each group are shown. Data are expressed as means ± SEM from four mice. *$p < 0.005$.

CD44$^-$ cells. Most CD62L$^-$CD44$^-$ cells showed a similar IL-7R/CD127 expression level to the other subsets; however, some cells within this subset showed a lower expression of the IL-7R as seen in Fig. 4 (arrow). These results indicate that the mechanism by which NK cells suppress CD62L$^-$CD44$^-$ T cells may be different from that by which they suppress T_{EM}, which is due to NK cell-induced apoptosis via Fas and/or DR5.

The lack of IL-7 does not affect the cytotoxic activity of NK cells

Because we have previously observed the upregulated annexin V and downregulated Bcl-2 expressions in the CD4$^+$ T cells transferred into IL-7$^{-/-}$RAG$^{-/-}$ recipients (10), we speculated that the ability of NK cells to suppress the T cells could be affected by the presence or absence of IL-7. We therefore performed a cytotoxicity assay to test this hypothesis. As expected, NK cells (effector) had negligible cytotoxicity toward CD62L$^+$CD44$^-$ naive T cells (target) derived from WT SP (T:E ratio, 1:5) regardless of whether rIL-7 was present (Fig. 5A). When CD62L$^-$CD44$^+$ T_{EM} derived from colonic LP of RAG$^{-/-}$ mice, which had been injected with naive T cells 12 wk previously, were coincubated with the NK cells (T:E ratio, 1:5), the mortality of the target cells was elevated but this cell-mediated cytotoxicity did not change in the presence of rIL-7 (Fig. 5B). These results suggested that the cytotoxic ability of NK cells derived from WT mice was not affected by IL-7 and further suggested that the susceptibility of T cells to the cytotoxic activity of NK cells was not changed by the presence of IL-7 using this assay. When increasing the ratio of CD62L$^-$CD44$^+$ T_{EM} (T:E ratio, 1:5 to 1:0.6), the mortality was decreased (Fig. 5C). These data suggest that the cytotoxicity is decreased when the number of target T cells exceeds the capacities of effector NK cells to suppress T cells. However, it was still unclear whether the cytotoxic ability of NK cells could be modulated during its development in vivo in the presence or absence of IL-7. Therefore, the cytotoxic ability of NK cells derived from RAG$^{-/-}$ and IL-7$^{-/-}$ RAG$^{-/-}$ mice was examined. As seen in Fig. 5D, there was little mortality of CD62L$^+$ CD44$^-$ naive T cells alone, and this mortality was unaffected even if coincubated with NK cells derived from either RAG$^{-/-}$ or IL-7$^{-/-}$RAG$^{-/-}$ mice (T:E ratio, 1:5). The mortality of CD62L$^-$CD44$^+$ T_{EM} was elevated compared with that of T_{EM} alone when coincubated with NK cells derived from RAG$^{-/-}$ mice and was similar to that following coincubation with NK cells derived from IL-7$^{-/-}$RAG$^{-/-}$ mice (T:E ratio, 1:5; Fig. 5E).

Additionally, the expression levels of NK receptors (30) that reflect the function of NK cells (Fig. 5F), as well as the levels of CD11b and CD27 that determine the differentiation status of NK cells (31) (Fig. 5G), were not altered in NK cells derived from IL-7$^{-/-}$RAG$^{-/-}$ mice, compared with those from RAG$^{-/-}$ mice.

To further demonstrate that there are no differences of NK cell functions between RAG$^{-/-}$ and IL-7$^{-/-}$RAG$^{-/-}$, we also measured the cytotoxic activities of these cells against YAC-1 cells using the [^{51}Cr] release assay, as well as the production of IFN-γ from these cells. As seen in Fig. 5H and 5I, neither the cytotoxicities against YAC-1 cells nor IFN-γ production of NK cells was modified in the IL-7$^{-/-}$RAG$^{-/-}$ mice when compared with

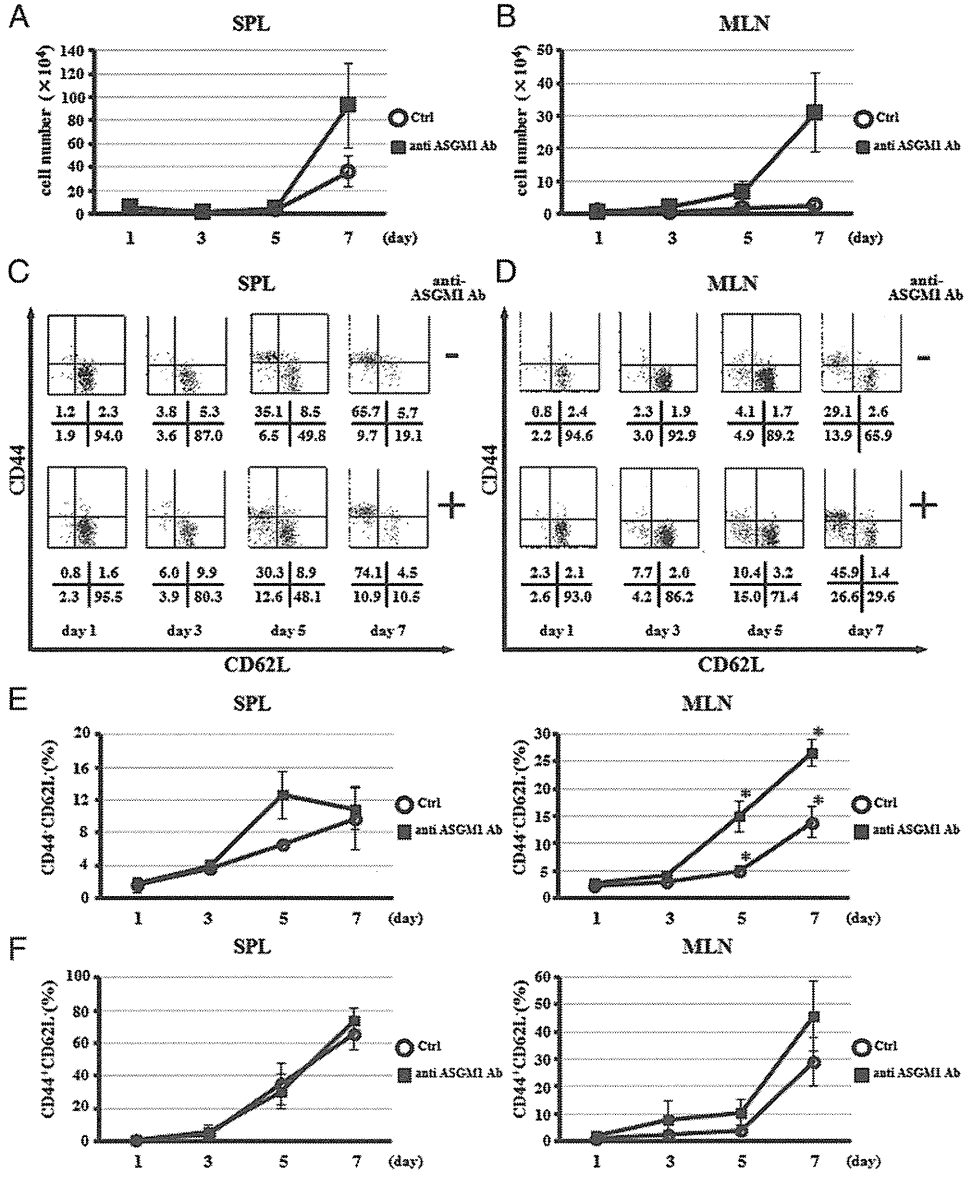

FIGURE 3. NK cell depletion results in the increase in $CD44^+CD62L^-$ and $CD44^-CD62L^-$ subsets in naive T cell-transferred $RAG^{-/-}$ mice. (**A** and **B**) Naive T cells derived from WT SP were adoptively transferred into $RAG^{-/-}$ mice that were preinjected with either vehicle control (○) or anti-ASGM1 Ab (■). Mice were sacrificed and the total number of $CD4^+$ T cells isolated from SP (A) or MLN (B) was counted. Cells were stained with PerCP-conjugated anti-CD3 and allophycocyanin-conjugated anti-CD4 Abs, and were then subjected to FACS to calculate the number of T cells in each sample. The number of $CD4^+$ T cells at the indicated time points is shown. Data are expressed as means ± SEM ($n = 4$). (**C** and **D**) The naive T cell-receiving $RAG^{-/-}$ mice that had been preinjected with either vehicle control or anti-ASGM1 Ab were sacrificed at the indicated time points after naive T cell transfer. The isolated lymphocytes from SP (C) or MLN (D) were stained with allophycocyanin-conjugated anti-CD4, PerCP-conjugated anti-CD3, FITC-conjugated anti-CD62L, and PE-conjugated anti-CD44 Abs and were subjected to FACS. Representative data from four experiments are shown. The numbers in each data quadrant indicate percentage of gated populations. (**E** and **F**) The percentage of $CD44^-CD62L^-$ cells in $RAG^{-/-}$ mice that received naive T cells with or without anti-ASGM1 Ab injection. Mice were sacrificed at the indicated time points, lymphocytes isolated from SP (E) or MLN (F) were stained with anti-CD3, anti-CD4, anti-CD62L, and anti-CD44 Abs and were then subjected to FACS to analyze the percentage of the subset. Data are expressed as means ± SEM from five experiments. $*p < 0.05$.

$RAG^{-/-}$ mice. These results confirm that a lack of IL-7 does not affect the cytotoxic activity of NK cells either in vitro or in vivo.

K cell depletion elicits severe colitis in naive T cell-transferred IL-7$^{-/-}$ RAG$^{-/-}$ recipient mice

We previously reported that the development of colitis is abrogated by a lack of IL-7. Given that NK cells can suppress T cells in vitro and in vivo independently of IL-7, we next assessed the influence of NK cells on colitis in the context of IL-7 deficiency in vivo. IL-$7^{-/-}$ $RAG^{-/-}$ mice were injected i.p. with naive T cells with or without anti-ASGM1 Ab treatment, and colitis was monitored after 12 wk (Fig. 6A). As previously observed, the induction of colitis was completely abrogated in vehicle control-injected IL-$7^{-/-}$$RAG^{-/-}$ mice, as shown by clinical and histological scores and cytokine production from colonic LP lymphocytes, although the presence of occasional leukocytes was observed in colonic tissues (Fig. 6B–E). However, when anti-ASGM1 Ab was injected, IL-$7^{-/-}$$RAG^{-/-}$ mice showed elicitation of colitis and similar severity of clinical phenotypes, such as wasting and diarrhea, as did the groups of $RAG^{-/-}$ recipients with or without anti-ASGM1 Ab treatment (Fig. 6B). Consistent with these findings, a significant deterioration in histological findings, such as mucosal damage, cell infil-

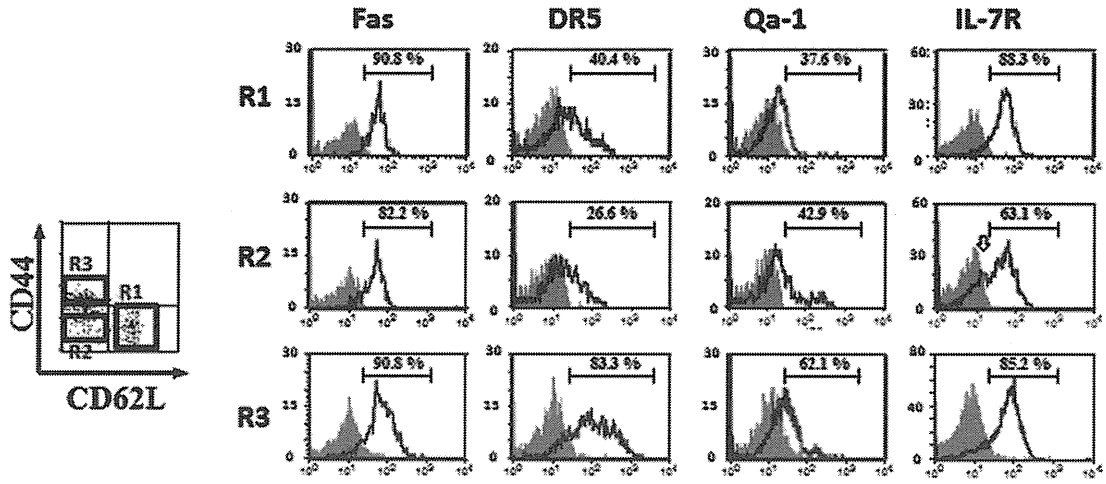

FIGURE 4. NK cells may target the $CD62L^-CD44^-$ subset by a different mechanism from that by which they target the $CD62L^-CD44^+$ subset. $RAG^{-/-}$ mice preinjected with anti-ASGM1 Ab were sacrificed 5 d after naive T cell transfer. Isolated splenocytes were stained with anti-CD62L, anti-CD44, and either anti-Fas, anti-DR5, anti-Qa1, or anti-CD127 Abs (open histograms) or isotype-matched control (filled histograms) and were then subjected to FACS. The populations within the appropriate gate on forward scatter and side scatter and either $CD62L^+CD44^-$ (naive, R1), $CD62L^-CD44^-$ (R2) or $CD62L^-CD44^+$ (T_{EM}, R3) were analyzed. Representative data from three experiments are shown.

tration, and crypt abscesses, was also observed in $IL\text{-}7^{-/-}RAG^{-/-}$ mice when treated with anti-ASGM1 Ab (Fig. 6C, 6D) in association with the exacerbation in the clinical scores of these mice. Moreover, the production of cytokines such as IFN-γ, TNF-α, and IL-17 by colonic LPL from anti-ASGM1 Ab-treated $IL\text{-}7^{-/-}RAG^{-/-}$ mice was significantly upregulated when compared with the vehicle control-treated group, despite the fact that their production was relatively lower than that of $RAG^{-/-}$ groups with or without anti-ASGM1 Ab treatment (Fig. 6E). These results suggest that severe inflammation occurs in colonic tissues following NK cell depletion even in $IL\text{-}7^{-/-}RAG^{-/-}$ mice.

Additionally, to confirm the activities of cells that had infiltrated the tissues, absolute numbers of splenic and colonic LP $CD4^+$ T cells isolated from these colitic mice were calculated (Fig. 7A) and analyzed by FACS (Fig. 7B, 7C). As seen in Fig. 7B and 7C, the percentage of $NK1.1^+$ cells in both SP and colonic LP was greatly decreased in T cell-reconstituted mice treated with anti-ASGM1 Ab. Note that the percentages of $NK1.1^+$ populations in both SP and colonic LP from T cell-reconstituted $IL\text{-}7^{-/-}RAG^{-/-}$ mice not treated with the anti-ASGM1 Ab were dramatically increased, because there were less $CD4^+$ T cells in the tissues (Fig. 7A). Additionally, $CD4^+$ T cells with a $CD44^+CD62L^-$ phenotype were observed in all mouse groups (Fig. 7B, 7C). However, the percentage of these cells was lower, especially in colonic LP, in $IL\text{-}7^{-/-}RAG^{-/-}$ recipient mice not treated with the anti-ASGM1 Ab relative to the other groups. Associated with this finding, the expression levels of IL-7R and CD69 in both splenic and colonic LP $CD4^+$ T cells from $IL\text{-}7^{-/-}RAG^{-/-}$ recipient mice not treated with the anti-ASGM1 Ab were downregulated relative to the other groups (Fig. 7B, 7C). However, treatment with the anti-ASGM1 Ab resulted in an increase in $CD4^+CD44^+CD62L^-$ T cells in both splenic and colonic LP, as well as upregulation of the expression of IL-7R and CD69 in $IL\text{-}7^{-/-}RAG^{-/-}$ recipient mice. These results indicate that the T cells reconstituted into $IL\text{-}7^{-/-}RAG^{-/-}$ recipient mice are still able to survive even 12 wk after injection, but that they somehow fail to differentiate sufficiently to induce colitis. Moreover, these data suggest that the depletion of NK cells in this context may assist the T cells to establish themselves as pathogenic T cells.

To further confirm whether such elicitation of pathogenic T cells in $IL\text{-}7^{-/-}RAG^{-/-}$ recipients was induced by NK cell depletion, anti-NK1.1 Ab was used for the same model. $IL\text{-}7^{-/-}RAG^{-/-}$ mice were injected i.p. with naive T cells with or without anti-NK1.1 Ab treatment, and colitis was monitored after 12 wk (Fig. 8A). The $IL\text{-}7^{-/-}RAG^{-/-}$ recipients injected with anti-NK1.1 Ab showed severe colitis (Fig. 8B–D) with increased production of proinflammatory cytokines by the colonic LPL when compared with the isotype control-injected mice (Fig. 8E). These results suggested that the phenotypes shown in $IL\text{-}7^{-/-}RAG^{-/-}$ recipients may reflect NK cell regulation of T cell development in this model.

NK cell depletion at an early stage is critical for the induction of colitis in naive T cell-transferred $IL\text{-}7^{-/-}RAG^{-/-}$ recipient mice

Because NK cell depletion resulted in the exacerbation of colitis even in $IL\text{-}7^{-/-}RAG^{-/-}$ recipient mice, we finally examined the effect of NK cell depletion at early and late stages of colitis development in $IL\text{-}7^{-/-}RAG^{-/-}$ recipient mice. Mice receiving naive T cells were also injected every 48 h with either the vehicle control for 12 wk (Ctrl), anti-ASGM1 Ab for 12 wk (0–12 wk), anti-ASGM1 Ab for 4 wk followed by vehicle control for 8 wk (0–4 wk), or vehicle control for 4 wk followed by 8 wk anti-ASGM1 Ab (4–12 wk), and colitis was monitored after 12 wk (Fig. 9A). Mice injected with anti-ASGM1 Ab for the first 4 wk, or for the entire 12 wk, showed significantly more severe clinical phenotypes of colitis than did the other groups (Fig. 9B), which was associated with thickening and shortening of the colon and splenomegaly (Fig. 9C). Severe inflammation of the colon, as judged by histological analysis, was also noticeably induced in these two groups (Fig. 9D, 9E). However, mice injected with the anti-ASGM1 Ab at a later stage failed to induce colitis, although minor clinical symptoms and infiltration of a few cells into the colon were occasionally observed (Fig. 9B–E). Moreover, these degrees of severity of colitis were consistent with cytokine production from colitic LP T cells, since significantly upregulated IFN-γ and TNF-α production was observed in the groups treated with the anti-ASGM1 Ab either at the beginning or throughout the entire period, but not in the group treated with the Ab only at the later stage (Fig. 9F). Note that the level of IL-17 production in mice treated for the entire period with anti-ASGM1 Ab was significantly higher than that of mice treated with the Ab only at the

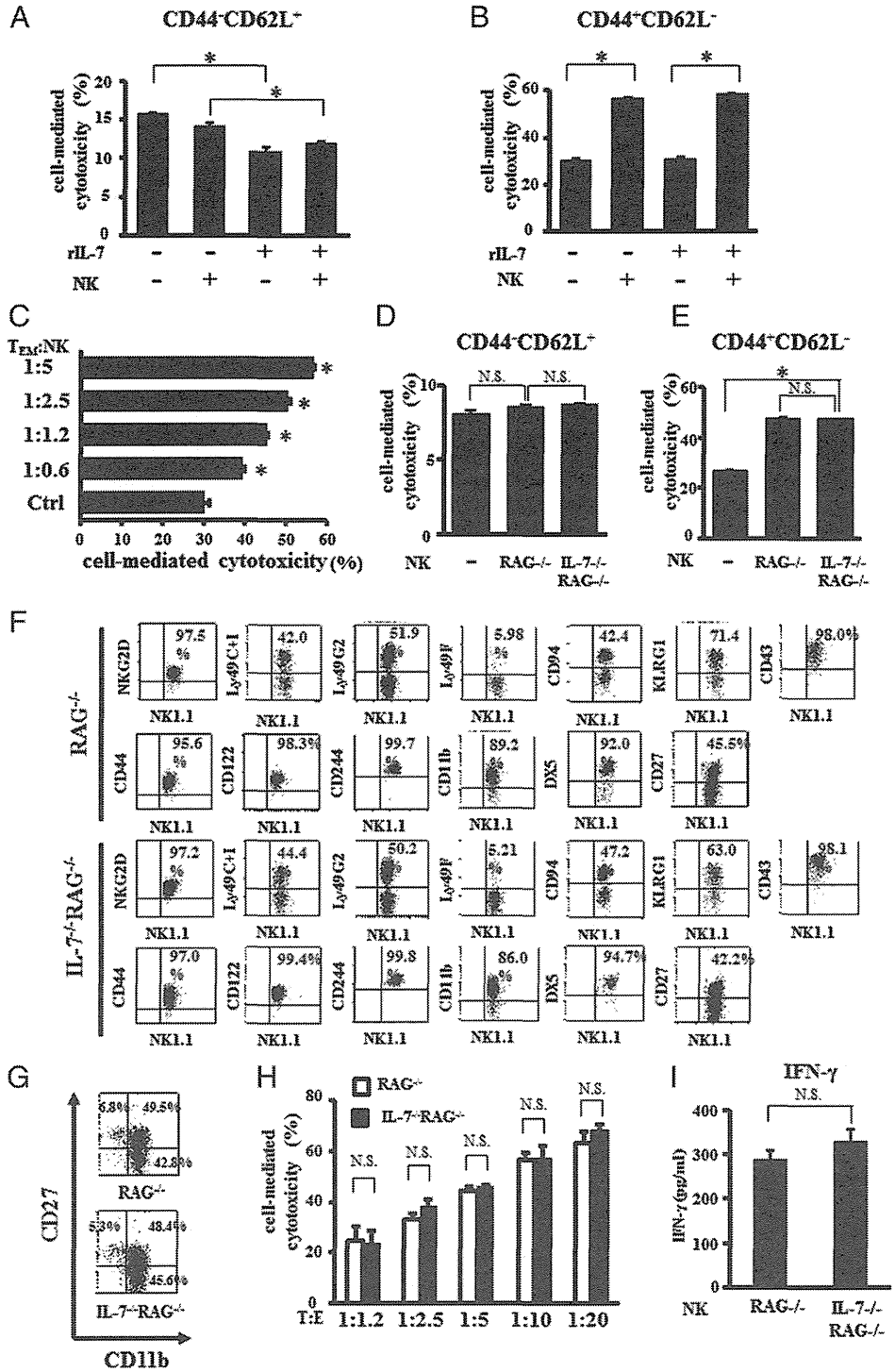

FIGURE 5. Cytotoxic activity of NK cells is not affected in the presence or absence of IL-7. (**A–C**) Splenic NK cells were isolated from WT mice by FACS sorting. Either $CD4^+CD62L^+CD44^-$ naive T cells isolated from WT SP (A) or $CD4^+CD62L^-CD44^+$ T_{EM} from colonic LP in $RAG^{-/-}$ mice that received naive T cells 12 wk previously (B and C) were stained with PKH2 and cocultured as target (T) cells with the isolated NK cells as effector (E) cells, in the presence or absence of IL-7 for 4 h. Cells were then harvested and stained with PI. The PKH2 and PI double-positive population is assumed to represent dead target cells (28). The mortality of target cells was calculated as the ratio of dead $PKH2^+$ cells. (A) T:E ratio, 1:5, with or without rIL-7; (B) T:E ratio, 1:5, with or without rIL-7; (C) T:E ratio, 1:5, 1:2.5, 1:1.25, or 1:0.625, without rIL-7. Control ($CD4^+$ T cells alone) is also shown as a negative control. Data are expressed as means ± SEM from three experiments. $*p < 0.001$. (**D** and **E**) Splenic NK cells were isolated from either $RAG^{-/-}$ or $IL\text{-}7^{-/-}$ $RAG1^{-/-}$ mice by FACS sorting. Either the $CD62L^+CD44^-$ naive T (D) or the $CD62L^-CD44^+$ T_{EM} (E) subset was stained with PKH2 and cocultured for 4 h with splenic NK cells derived from either $RAG^{-/-}$ or $IL\text{-}7^{-/-}RAG1^{-/-}$ mice. Cells were then stained with PI and subjected to the cytotoxic assay described above. Data are expressed as means ± SEM from three experiments. $*p < 0.001$. (**F**) Splenic NK cells were isolated from $RAG^{-/-}$ and $IL\text{-}7^{-/-}$ $RAG^{-/-}$ mice, and the expression of each NK receptor on these cells was assessed by FACS. The numbers indicate the percentage of cells positive for each NK receptor in the NK1.1-positive population. (**G**) Splenic NK cells isolated from either $RAG^{-/-}$ or $IL\text{-}7^{-/-}RAG^{-/-}$ mice were stained with anti-CD11b and anti-CD27 Abs and were then subjected to FACS to evaluate their differentiation status. The numbers indicate the quadrant percentages of each differentiation status in the NK1.1-positive population. (**H**) Splenic NK cells were isolated from $RAG^{-/-}$ (open) and $IL\text{-}7^{-/-}$ $RAG^{-/-}$ (filled) mice by FACS sorting. YAC-1 cells were labeled with $Na_2[^{51}Cr]O_4$ and cocultured as target (T) cells with the isolated NK cells as *(Figure legend continues)*

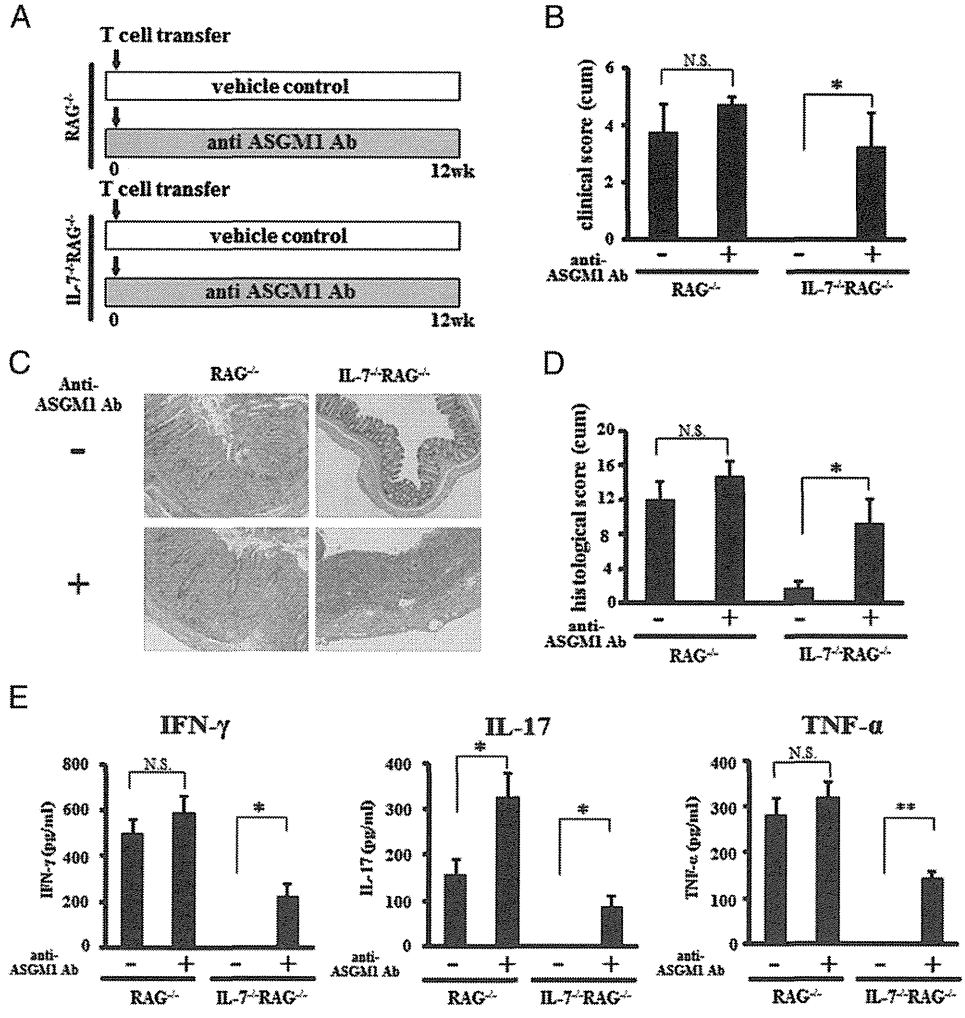

FIGURE 6. NK cell depletion with anti-ASGM1 Ab in naive T cell-receiving IL-7$^{-/-}$RAG$^{-/-}$ mice, as well as in RAG$^{-/-}$ recipients, results in the development of colitis. (**A**) Protocol for NK cell depletion in a colitis setting. Naive T cell-receiving RAG$^{-/-}$ and IL-7$^{-/-}$RAG$^{-/-}$ mice were injected with either anti-ASGM1 Ab (0–12 wk) or vehicle control (Ctrl) every second day for 12 wk starting from the day before adoptive transfer of naive T cells. (**B**) Clinical scores of each group are shown. Data are expressed as means ± SEM from four mice. *$p <$ 0.05. (**C**) Histological features of colons from naive T cell-transferred RAG$^{-/-}$ and IL-7$^{-/-}$RAG$^{-/-}$ recipients injected with either vehicle control (Ctrl) or anti-ASGM1 for 12 wk (0–12 wk). Representative features from four experiments are shown. (**D**) Histological scores of each group are shown. Data are expressed as means ± SEM from four mice. *$p < 0.05$. (**E**) Cytokine production by LP T cells from each group is shown. Concentrations of IFN-γ (*left*), TNF (*middle*), and IL-17 (*right*) in the culture supernatant are measured by ELISA. Data are indicated as means ± SEM from four samples. *$p < 0.05$, **$p <$ 0.01.

beginning (Fig. 9F), although there was no significant difference in either clinical or histological scores between these groups (Fig. 9B, 9E). These results suggest that NK cell depletion at the early stage, but not the late stage, of T_{EM} development is critical for the induction of colitis in IL-7$^{-/-}$RAG$^{-/-}$ recipient mice.

Discussion

We previously reported that adoptively transferred WT naive T cells injected into IL-7$^{-/-}$RAG$^{-/-}$ mice interestingly failed to induce colitis (10). However, it is known that IL-7 is not required for the in vitro differentiation of naive T cells into Th1 or Th17 cells (12). We therefore speculated that the reason why the IL-7$^{-/-}$RAG$^{-/-}$ mice that received naive T cells failed to maintain colitogenic CD4$^+$ T_{EM} may be associated not only with a lack of IL-7, but also with another mechanism that involves suppression of the primary stage of T_{EM} development in the recipients. We previously reported that apoptosis is preferentially induced in CD4$^+$ T cells when IL-7 is lacking in vivo. Thus, increased numbers of annexin V$^+$CD4$^+$ T cells were observed in IL-7$^{-/-}$RAG$^{-/-}$ recipient mice, into which these T cells had been adoptively transferred, compared with CD4$^+$ T cells in RAG$^{-/-}$ recipient mice (10). These data suggested that T cell suppression via apoptosis is a mechanism by which colitis is abrogated in IL-7$^{-/-}$RAG$^{-/-}$ recipient mice. We therefore determined whether NK cells, which are known to induce apoptosis in CD4$^+$ T cells, may play a role in such T cell suppression.

Several reports have suggested that NK cells suppress the inflammation caused by autoimmune responses not only in animal models such as EAE and collagen-induced arthritis, but also in clinical samples from patients with multiple sclerosis and systemic lupus erythematosus in humans (20–22, 28, 32, 33). For example, depletion of NK cells using Abs against NK1.1 or ASGM1 results in disease exacerbation in the EAE model (22, 28). Additionally, it has also been reported that NK cell depletion exacerbates an animal model of colitis, although the details underlying the mechanism have not been elucidated (24).

In the present study, NK cells were depleted in the naive T cell adoptively transferred colitis model to analyze the role of NK cells in this model. RAG$^{-/-}$ and IL-7$^{-/-}$RAG$^{-/-}$ mice that had received naive T cells were depleted of NK cells using an anti-ASGM1 (Figs. 1, 2, 6, 9, Supplemental Figs. 1, 2). However, it was of concern that ASGM1 may be expressed not only in NK cells but also in some subsets of T cells and macrophages when activated (34). Therefore, we also administered anti-NK1.1 Ab

effector (E) cells for 4 h. T:E ratio, 1:20, 1:10, 1:5, 1:2.5, or 1:1.25. Data are expressed as means ± SEM from three experiments. (**I**) Cytokine production by NK cells from each group is shown. Concentrations of IFN-γ in the culture supernatant are measured by ELISA. Data are indicated as means ± SEM from four samples.

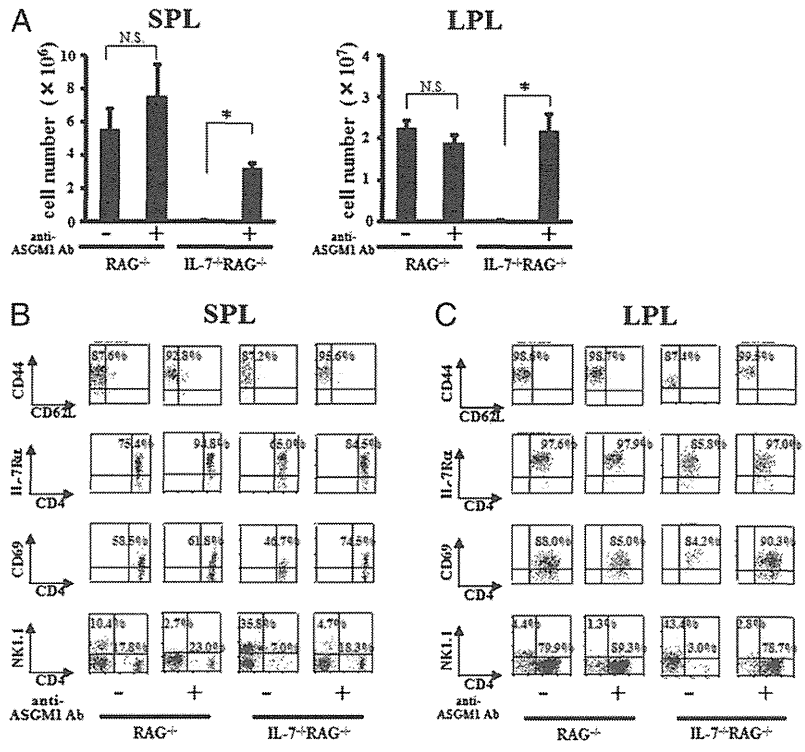

FIGURE 7. Colitogenic T_{EM} are induced in naive T cell-receiving IL-$7^{-/-}$RAG$^{-/-}$ by NK cell depletion. (**A**) Absolute numbers of $CD4^+$ T cells are shown. $CD4^+$ SPL (*left*) or colonic LPL (*right*) were isolated from naive T cell-receiving RAG$^{-/-}$ and IL-$7^{-/-}$ RAG$^{-/-}$ mice injected with either vehicle control (−) or anti-ASGM1 Ab (+) for 12 wk. Data are expressed as means ± SEM from five mice. *$p < 0.001$. (**B** and **C**) Isolated SPL (B) or colonic LPL (C) were stained with anti-CD4 and either anti-CD44, anti-CD127/IL-7Rα, anti-CD69, or anti-NK1.1 Abs and were then subjected to FACS analysis. Representative data from four experiments are shown.

using another experimental approach to confirm that the phenotypes shown in this model were induced by NK cell depletion (Fig. 8). Note that administration of anti-ASGM1 without T cell reconstitution to the IL-$7^{-/-}$RAG$^{-/-}$ mice does not trigger any inflammation in the colon (Supplemental Fig. 2). Also note that the appropriate controls, such as the same amount of rabbit Ig as a control for anti-ASGM1 polyclonal Ab and mouse IgG2a as an isotype-matched control for anti-NK1.1 (PK136), respectively, do not induce colitis in the recipients either (Figs. 2, 8, Supplemental Fig. 2). Interestingly, NK cell depletion at an early stage during colitis induction resulted in exacerbated colitis in the recipient, even in IL-$7^{-/-}$ RAG$^{-/-}$ recipient mice, in association with increased clinical and histological scores as well as upregulated cytokine production by colonic LP T cells. We observed strong

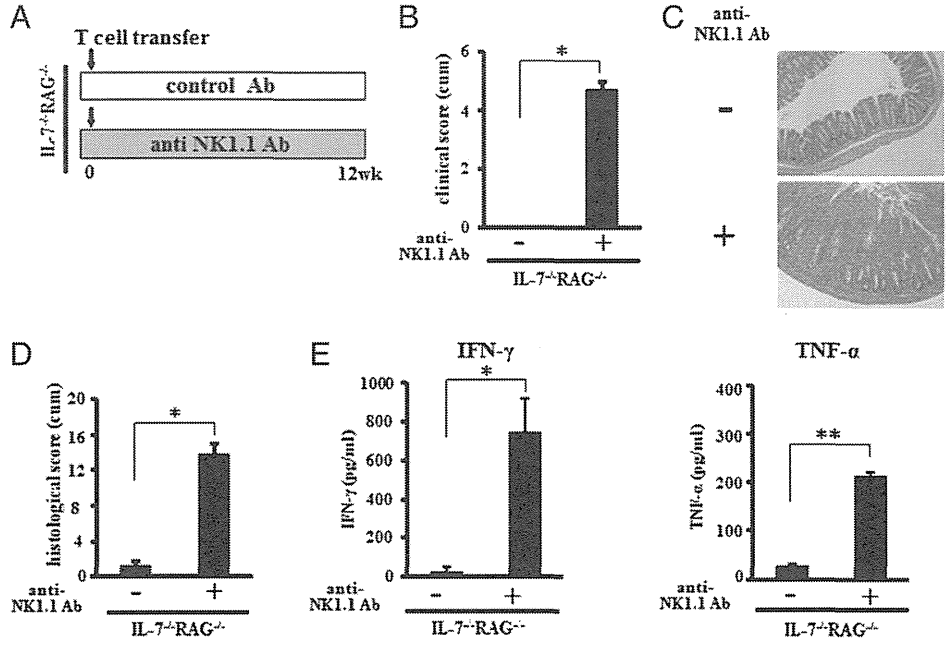

FIGURE 8. NK cell depletion with anti-NK1.1 Ab in naive T cell-receiving IL-$7^{-/-}$RAG$^{-/-}$ mice results in the elicitaion of colitis. (**A**) Protocol for NK cell depletion in a chronic colitis setting. IL-$7^{-/-}$RAG$^{-/-}$ mice receiving naive T cells were injected with either 0.5 mg/mouse anti-NK1.1 Ab or isotype control every second day for 12 wk. (**B**) Clinical scores of each group are shown. Data are expressed as means ± SEM from five mice. *$p < 0.001$. (**C**) Histological feature of colons from naive T cell-transferred IL-$7^{-/-}$RAG$^{-/-}$ recipients injected with isotype control (−, *top*) or anti-NK1.1 Ab (+, *bottom*). Representative features from each group are shown. (**D**) Histological scores of each group are shown. Data are expressed as means ± SEM from five mice. *$p < 0.001$. (**E**) Cytokine production by LP T cells from each group is shown. Concentrations of IFN-γ (*left*) and TNF-α (*right*) in the culture supernatant were measured by ELISA. Data are indicated as means ± SEM from five samples. *$p < 0.05$, **$p < 0.001$.